NSI RRC KI 90-12/1-01-02

ANALYSIS OF SPATIAL EFFECTS FOR ROD EJECTION ACCIDENTS IN A PWR

A.Avvakumov, V.Malofeev, and V.Sidorov

Date Published - January, 2002

NUCLEAR SAFETY INSTITUTE OF RUSSIAN RESEARCH CENTRE
''KURCHATOV INSTITUTE''
Kurchatov square 1
Moscow, Russia

ABSTRACT

Spatial effects in rod ejection accidents that are the design-basis events for a pressurized water reactor are analyzed in this study. Four cases for the Three Mile Island Unit 1 (TMI-1) model are considered: ejection of the central or peripheral control rod at the end of cycle or the beginning of cycle. Calculations were carried out using the RELAP-BARS code, which allows 3-D pin-by-pin neutronics and assembly-by-assembly thermal-hydraulics simulation of a transient. The results showed that the major parameters of a transient (the peak power and core energy deposition) were a function of spatial effects. An analysis of a dependence of the peak local fuel enthalpy on spatial effects was performed.

TABLE OF CONTENTS

Page

LIST OF FIGURES

LIST OF TABLES

1. INTRODUCTION

The objective of this study was to analyze spatial effects in the course of rod ejection accidents (REAs) with withdrawal of the central or off-central control rod. The rod ejection accident is the design-basis reactivity initiated event for a pressurized water reactor (PWR). The rod ejection scenario assumes a mechanical failure of the control rod drive mechanism and, as a result, ejection of a control rod to a fully withdrawal position due to the reactor coolant system pressure. The ejected rod worth must be sufficient to initiate a fast power excursion, otherwise the transient will be a very mild with a rather gradual energy deposition rise, and, thereof – out of interest. If a rapid power excursion occurs, then after a while (within a few hundredths of a second) it is terminated by the negative fuel temperature (Doppler) feedback.

From the point of view of a nuclear power plant safety analysis, peak local fuel enthalpy is a key parameter used as the acceptance criterion for unacceptable fuel damage in the course of reactivity initiated events in LWRs. It is clear that local fuel enthalpy depends on a spatial distribution of the energy deposition in the core during the accident and, therefore, to determine a peak value of this parameter properly it is necessary to consider 3 D pin-by-pin neutronic model. In best-estimate nodal diffusion methods such a problem is usually split into two steps: first – a calculation of assembly-average power distribution, and second one – peak power estimate within selected fuel assemblies by a pin-by-pin reconstruction method with further estimate of the peak local fuel enthalpy. This procedure has evident drawbacks compared with the direct pin-by-pin methods, especially when spatial effects are very complicated during the event.

Analysis of a REA, as a rule, involves the following parameters of interest: the core peak power and the energy deposition, which can be approximately related to the fuel enthalpy rise under the assumption of an adiabatic process (i.e. no heat transfer to the coolant). A simple analytical approximation, based on the Nordheim-Fuchs model, allows to establish dependence of the peak power, pulse width and energy deposition on several parameters: the inserted reactivity (rod worth), delayed neutron fraction, prompt neutron lifetime, and a parameter which characterizes the Doppler feedback. As it was found the magnitude of the last parameter depended strongly on spatial effects during a transient.

It is well-established that spatial effects play an important role in the REA consequences of interest. These effects are revealed in a dual manner. On the one hand, the higher the power peaking factor, the higher the local energy deposition and, consequently, the local fuel temperature (or enthalpy) increase. On the other hand, it is well-known that the Doppler feedback is stronger in the hottest fuel regions and reduces the peak power and reactivity. Besides, local heating of the coolant also decreases the peak power and reactivity.

The REA analyses were performed using the RELAP–BARS code [1], which allows a 3-D pin-by-pin neutronics and assembly-by-assembly thermal-hydraulics simulation of a light water reactor (LWR). Calculations were carried out for four PWR REAs with ejection of the central or peripheral control rod at the end of cycle (EOC) or the beginning of cycle (BOC). To provide maximum non-uniformity of the power distribution in axial direction, all control rods were either fully inserted in the core or fully withdrawn during a transient.

A PWR calculational model has 1/8 radial symmetry and includes fuel assemblies with different properties surrounded by the radial reflector. In an axial direction a uniform core nodalization scheme (axial layers with different properties) is used with the top and bottom reflectors. Although the BARS code allows a continuous axial distribution of power (due to use of the Fourier series expansion), hereinafter an axial power distribution is given in terms of used nodalization scheme (for the simplicity in a code intercomparison).

In this study the following parameter is used to characterize spatial effects in the REAs: the total power peaking factor, F_q, defined as a ratio between the maximum fuel pellet power and an average pellet power over the core. It should be noted that “fuel pellet” term in this study is related to a calculational axial node, which is generally larger compared with the actual height of a fuel pellet. This definition of the power peaking factor is valid for the pin-by-pin approach. In an assembly-by-assembly representation the following definition of the power peaking factor, $F_q^{'}$, is used: it is a ratio between the maximum power in an axial node of the hottest assembly to an average node power (provided that uniform axial nodalization is used).

Section 2 focuses on the analysis of the RELAP–BARS calculational results for considered transients. This section also contains descriptions of the calculational models. In Section 3 the Nordheim-Fuchs model is used to understand the role of spatial effects on the major parameters of a REA. Evaluations of the feedback parameter as a function of the power peaking factor are derived. Section 4 provides a comparison of the rod worth steady-state calculations performed by different codes and possible uncertainties in the REA parameters due to uncertainty in the rod worth prediction. Appendix A contains the calculational results obtained by RELAP–BARS during modeling of a REA with ejection of the central rod with increased worth at EOC conditions.

2. ANALYSIS OF ROD EJECTION ACCIDENTS

The reactor model was based on Three Mile Island Unit 1 (TMI-1) used as an international benchmark exercise [2]. The reference design for the PWR is derived from the reactor geometry and operational data of the TMI-1 NPP. Two different cores were used in this study. First core is assumed to be at the end of cycle (EOC), with a boron concentration in the coolant of 5 ppm, and equilibrium Xe and Sm concentration. The average burnup in the core is 40.7 GWd/t (the maximum burnup is about 58 GWd/t). Detailed specifications for this core are given in [2]. Another core is assumed to be at the beginning of cycle (BOC) with the average core exposure of 18.2 GWd/t and boron concentration of 1700 ppm [3]. The hot zero power (HZP) conditions are defined as follows: the reactor power is 2772 W (10^{-6} of rated power), fuel/coolant temperature is 551 K and core inlet pressure is 15.4 MPa. The reactor has one-eight core symmetry, as Figures 2.1 and 2.2 show. Initial steady-states are the same for both cores: control rod banks 1 to 4 are completely withdrawn, banks 5 to 7 are completely inserted. Figures 2.1 and 2.2 show only inserted control rod banks. For the simplicity it was assumed that the delayed neutron fraction was 521.10 pcm at EOC and 632.34 pcm at BOC.

A control rod cluster of Bank 7 is ejected from the core centre (Assembly H8) or periphery (Assembly N12) during 0.1 s to initiate a transient, which lasts 2.5 seconds. This duration was chosen from the previous analysis of the rod ejection accidents where it was found that the fuel enthalpy increase has to be terminated due to the reactor trip up to this moment [4]. In this study no reactor scram was assumed. Thus, four cases were studied: two types of REA (the central or peripheral rod ejection) at two initial conditions (EOC or BOC).

Steady-state calculations show that an actual worth of the ejected rod is lower compared with the delayed neutron fraction, β. Table 2.1 presents the calculational results obtained by the BARS code at EOC [5] and BOC. It is obvious, that these magnitudes are insufficient to reach prompt critical. Since a power excursion below prompt critical is out of interest, the control rod worth in each case of this study was fixed at 1.21β. This worth is possible only when there is a large distortion of flux distribution over the core: for instance, if the control rod at position M11 is out of the core throughout the transient with ejection of the peripheral control rod at position N12. Thus, to provide 1.21β worth of the ejected rod, the initial core conditions have to be changed. In cases of the central rod ejection there were changes in neutronic parameters of the ejected rod. When the peripheral rod was ejected, the control rod in Assembly M11 was assumed to be stuck out of the core and the ejected rod was partly inserted to the core to provide required 1.21β worth.

	8	9	10	11	12	13	14	15
H	52.86 Bank 7	30.19	56.25	30.85	49.53 Bank 7	28.11	53.86 Bank 6	55.78
K		57.94	30.80	55.43	29.83	53.95 Bank 5	25.55	49.17
L			57.57 Bank 6	30.22	54.40	27.86	23.30	47.30
M				49.71 Bank 5	28.85	52.85	40.94	
N					48.75 Bank 7	23.86	41.45	
O						37.34		

52.86	- fuel burnup (GWd/t)
Bank 7	- No. of regulating bank

Figure 2.1. One-Eight Core Layout (EOC Initial Conditions)

	8	9	10	11	12	13	14	15
H	30.69 Bank 7	0.16 Gd + B	29.50	0.18 Gd + B	24.53 Bank 7	0.16 Gd + B	36.51 Bank 6	48.20
K		32.26	0.17 Gd + B	29.30	0.17 Gd + B	29.25 Bank 5	0.15 Gd + Gd	40.34
L			31.69 Bank 6	0.18 Gd + B	30.12	0.17 Gd + B	0.14	39.62
M				24.52 Bank 5	0.18 B	31.73	26.73	
N					24.89 Bank 7	0.17	32.22	
O						24.82		

30.69	- fuel burnup (GWd/t)
Bank 7	- No. of regulating bank

Gd	- 4 fuel pins with Gd
B	- B_4C burnable poison rods

Figure 2.2. One-Eight Core Layout (BOC Initial Conditions)

Table 2.1. Steady-State Calculation Results for Rod Worths

Case Index	Rod Position	Delayed Neutron Fraction, β (pcm)	Rod Worth (pcm / β)
EOC Centre	Assembly H8	521.10	349.3 / 0.670
EOC Periphery	Assembly N12	521.10	472.8 / 0.907
BOC Centre	Assembly H8	632.34	273.5 / 0.432
BOC Periphery	Assembly N12	632.34	548.5 / 0.867

Due to different delayed neutron fractions at EOC and BOC, an assumption of 1.21β worth means that the absolute value of the rod worth at BOC is greater by 21% compared with the EOC cases. For this reason it can be expected in this study that consequences of BOC REAs are to be more severe in terms of fuel enthalpy. (To compare the results for EOC REA with the same absolute value of the rod worth as at BOC, i.e. 1.47β, an additional calculation was carried out for the central rod ejection. The calculational results are given in Appendix A.)

Because of the REA start-up conditions corresponded to HZP with homogeneous thermal-hydraulic characteristics over the core, the RELAP thermal-hydraulics input deck was the same in all cases. An assembly-average representation of fuel and coolant parameters with 24 axial nodes was used to treat the core thermal-hydraulics. Besides, in each calculation a separate heat structure was chosen to represent the hottest fuel pin in the reactor core. The coolant thermal-hydraulic parameters for this heat structure corresponded to those for an assembly where the hottest pin was located.

The following features were investigated: core power and reactivity, fuel assembly powers, temperatures and enthalpies including their local values. Table 2.2 presents major core parameters of four REAs calculated by RELAP–BARS. The peak values of fuel temperature and enthalpy occur at the end of the transient (2.5 s). Total fuel enthalpy may be defined by adding the initial value of about 17 cal/g. Position of the hottest pins within a 15×15 PWR standard fuel assembly (FA) is given in Figure 2.3. Axial position of the hottest fuel pellet is given in terms of axial nodes (totally 24) from the bottom of the core. The core height is 357.12 cm, therefore, the node size is 14.88 cm. Thus, Node 22 is located between 312.5 cm and 327.4 cm from the core bottom. In the BOC cases the hottest pellet is located between Nodes 19 and 20, i.e. between 267.8 and 297.6 cm. The power peaking factors (total, F_q, radial, F_r, and axial, F_z) are given at 0.15-0.2 s (when they reach their maximum values) and at the end of the transient (2.5 s).

Table 2.2. Core Parameters in REAs

Case Index →	EOC Centre	EOC Periphery	BOC Centre	BOC Periphery
Ejected Rod Worth (pcm / β)	630.9 / 1.2107	631.0 / 1.2109	765.7 / 1.2109	765.7 / 1.2108
Peak Power (GW / % Nominal)	11.05 / 398.6	4.39 / 158.2	37.49 / 1352.5	13.07 / 471.4
Time of Peak Power (ms)	335.9	298.2	254.2	243.0
Power Pulse Width (ms)	61.9	64.5	39.8	41.4
Core-Average Fuel Temperature (K)	590.2	568.8	664.3	594.9
Maximum FA Temperature (K)	812.0	785.6	898.9	898.0
Maximum Fuel Pin Temperature (K)	835.3	851.6	935.9	996.1
Maximum FA Enthalpy Increase (cal/g)	18.88	16.87	25.52	25.45
Max. Pin Enthalpy Increase (cal/g)	20.65	21.90	28.37	33.04
Position of the Hottest Assembly	H9	M12	H9	N13
Position of the Hottest Fuel Pellet	H9 Node 22	N13 Node 22	H9 Nodes 19, 20	N13 Nodes 19, 20
Pin-by-Pin Total Peaking Factor, F_q	8.04 / 6.51	20.1 / 16.2	4.11 / 3.09	12.9 / 9.52
Assembly-Average Peaking Factor, F_q'	7.42 / 6.03	16.0 / 13.0	3.71 / 2.79	10.2 / 7.51
Pin-by-Pin Radial Peaking Factor, F_r	2.91 / 2.66	7.42 / 6.61	2.73 / 2.48	8.76 / 7.40
Assembly-Average Peaking Factor, F_r'	2.68 / 2.46	5.93 / 5.32	2.46 / 2.24	6.91 / 5.83
Average Axial Peaking Factor, F_z	2.76 / 2.45	2.71 / 2.44	1.50 / 1.25	1.47 / 1.29

					R				R					
			R	2							R			
			2,4											
1		R			R				R			R		
							3							
						3	C	3						
							3							
1		R			R				R			R		
			2											
			R								R			
					R				R					

R - control rod guide tube

C - instrumentation tube

1 - EOC Centre

2 - EOC Periphery

3 - BOC Centre

4 - BOC Periphery

Figure 2.3. Position of the Hottest Pins in Fuel Assembly during REAs

Figures 2.4 through 2.7 give assembly-average power distributions obtained in four REAs at time when the core power reaches its maximum and at the end of the transient (2.5 s). All distributions are normalized to an average value and, therefore, the maximum value shows the assembly-average radial peaking factor (at the end of the transient they coincide with those given in Table 2.2).

A comparison between the assembly-average and pin-by-pin radial peaking factors shows about 10%-difference in the cases with ejection of the central rod and more then 25%-difference in the cases with ejection of the peripheral rod. It is very important in regard to definition of the hottest fuel pin by indirect methods, such as a flux reconstruction, in assembly-by-assembly calculations. Since the peripheral fuel assemblies have, as a rule, higher intra-assembly power peaking factor, it is of interest to consider them from the point of view of intra-assembly power distribution. For instance, in Case EOC Periphery it was found that in the vicinity of the ejected rod (position N12) there were 5 hot fuel assemblies: N12 and two symmetrical N13 and M12. Their mean powers were within 5%-uncertainty. In spite of the fact that the last assembly had the peak power, the hottest fuel pin belonged to Assembly N13, diagonally adjacent to the core reflector. In turn, the intra-assembly peaking factor for this assembly was 1.26 whereas for the rest of the hot assemblies it was 1.11. As a result, 15%-underestimation in fuel enthalpy increase for the hottest fuel pin can occur only due to incorrect definition of its position.

For this study with relatively simple scenario of the transient starting from HZP, it was not so difficult to define the hottest pins in advance. It is clear, that as can be seen in Figures 2.1 and 2.2, in the cases with ejection of the central rod the hottest pins have to be located in Assembly H9 (adjacent to Assembly H8) with relatively low fuel burnup. Analogously, in cases with ejection of the peripheral rod the hottest pins are to be located somewhere in Assemblies M12, N13 or even N12 with the highest powers. But in many other cases with rather complicated spatial power distribution history, the flux reconstruction procedure may encounter serious difficulties. Another problem is use of this procedure for the peripheral assemblies adjacent to the core reflector where the flux reconstruction method may lead to significant uncertainty in pin powers.

Core-average axial power distributions are given in Figure 2.8 for two cases with ejection of the central rod at EOC and BOC at two time moments: 0.2 s and the end of the transient. It can be seen from Figures 2.4 through 2.8 and the data presented in Table 2.2, that the power peaking factor decreases due to the core heat-up during the transient: by 20% at EOC and by 25% at BOC.

	8	9	10	11	12	13	14	15
H	2.070 1.926	2.631 2.463	1.857 1.756	1.710 1.646	0.649 0.641	0.757 0.774	0.336 0.352	0.236 0.249
K		1.950 1.830	1.982 1.884	1.338 1.296	1.222 1.218	0.561 0.576	0.835 0.876	0.334 0.353
L			0.874 0.841	1.321 1.301	1.091 1.103	1.215 1.257	1.002 1.054	0.351 0.372
M				0.634 0.638	1.128 1.159	0.938 0.976	0.699 0.736	
N					0.617 0.642	0.986 1.038	0.457 0.483	
O						0.564 0.597		

$t = t_{max}$ →
$t = 2.5$ s →

2.631 2.463

- FA with peak power and the hottest pin

Figure 2.4. Power Distributions (Case EOC Centre)

		4	5	6	7	8	9	10	11	12	13	14	15
				0.068 0.096	0.068 0.094	0.056 0.075	0.091 0.119	0.101 0.131					
		0.083 0.119	0.132 0.186	0.197 0.274	0.174 0.238	0.082 0.109	0.234 0.303	0.300 0.385	0.226 0.285	0.162 0.201			
	0.102 0.146	0.182 0.258	0.182 0.253	0.249 0.339	0.126 0.167	0.198 0.253	0.167 0.210	0.389 0.486	0.324 0.401	0.378 0.461	0.243 0.291		
		0.119 0.165	0.232 0.314	0.244 0.320	0.305 0.386	0.186 0.228	0.394 0.477	0.382 0.461	0.436 0.522	0.277 0.325	0.491 0.571	0.243 0.280	
			0.142 0.186	0.326 0.411	0.367 0.447	0.527 0.625	0.466 0.544	0.525 0.606	0.305 0.345	0.622 0.700	0.551 0.619	0.436 0.489	
				0.237 0.287	0.582 0.685	0.608 0.698	0.771 0.864	0.431 0.471	0.804 0.867	0.724 0.783	0.845 0.921	0.741 0.808	0.275 0.298
					0.590 0.675	0.870 0.966	0.874 0.937	1.215 1.271	1.012 1.047	1.035 1.071	0.522 0.541	0.798 0.835	0.334 0.348
H						0.544 0.580	1.418 1.465	1.450 1.464	1.772 1.759	0.853 0.833	1.181 1.149	0.570 0.554	0.408 0.398
K							1.454 1.461	2.152 2.111	2.150 2.059	2.610 2.458	1.404 1.314	2.202 2.067	0.863 0.813
L								1.544 1.474	3.700 3.465	3.583 3.310	4.108 3.789	3.229 2.998	1.069 0.998
M									4.042 3.726	5.792 5.316	4.221 3.856	2.787 2.564	
N										5.506 5.011	5.734 5.241	2.257 2.067	
O							$t = t_{max}$ → $t = 2.5$ s →				3.343 3.050		

5.792 5.316	- FA with peak power
5.734 5.241	- FA with the hottest pin

Figure 2.5. Power Distributions (Case EOC Periphery)

	8	9	10	11	12	13	14	15
H	1.847 1.712	2.409 2.237	1.969 1.844	1.694 1.620	0.713 0.709	0.736 0.758	0.330 0.349	0.169 0.180
K		1.979 1.840	1.942 1.831	1.431 1.377	1.180 1.178	0.617 0.637	0.857 0.906	0.258 0.275
L			0.983 0.943	1.301 1.278	1.072 1.085	1.141 1.184	1.046 1.105	0.280 0.298
M				0.717 0.726	1.135 1.170	0.954 0.996	0.630 0.666	
N					0.744 0.780	1.138 1.201	0.406 0.431	
O						0.572 0.608		

$t = t_{max}$ →
$t = 2.5$ s →

2.409 2.237

- FA with peak power and the hottest pin

Figure 2.6. Power Distributions (Case BOC Centre)

		4	5	6	7	8	9	10	11	12	13	14	15
				0.053 0.080	0.051 0.076	0.039 0.056	0.068 0.095	0.078 0.108					
		0.072 0.110	0.116 0.175	0.200 0.300	0.174 0.257	0.079 0.112	0.234 0.323	0.303 0.415	0.196 0.264	0.139 0.183			
	0.100 0.154	0.203 0.311	0.180 0.269	0.230 0.336	0.137 0.195	0.190 0.260	0.180 0.241	0.355 0.472	0.321 0.420	0.417 0.540	0.230 0.293		
		0.138 0.208	0.229 0.333	0.239 0.335	0.297 0.400	0.205 0.268	0.379 0.485	0.370 0.472	0.427 0.540	0.313 0.390	0.519 0.640	0.197 0.240	
			0.160 0.224	0.326 0.436	0.402 0.517	0.535 0.668	0.506 0.620	0.517 0.626	0.333 0.397	0.586 0.693	0.519 0.612	0.366 0.429	
				0.274 0.351	0.594 0.735	0.673 0.810	0.782 0.914	0.490 0.555	0.775 0.865	0.682 0.765	0.754 0.853	0.730 0.825	0.204 0.230
					0.637 0.765	0.861 0.997	0.938 1.040	1.216 1.307	1.073 1.137	0.976 1.037	0.552 0.588	0.772 0.831	0.240 0.258
H						0.570 0.628	1.398 1.477	1.574 1.617	1.736 1.746	0.911 0.900	1.112 1.089	0.543 0.530	0.284 0.278
K							1.551 1.579	2.132 2.104	2.241 2.143	2.433 2.271	1.505 1.392	2.227 2.062	0.661 0.616
L								1.709 1.623	3.530 3.253	3.453 3.119	3.810 3.429	3.328 3.022	0.847 0.778
M									4.258 3.815	5.795 5.120	4.360 3.844	2.528 2.256	
N										6.293 5.504	6.669 5.833	2.052 1.809	
O											3.408 2.981		

$t = t_{max}$ →

$t = 2.5$ s →

6.669 5.833

- FA with peak power and the hottest pin

Figure 2.7. Power Distributions (Case BOC Periphery)

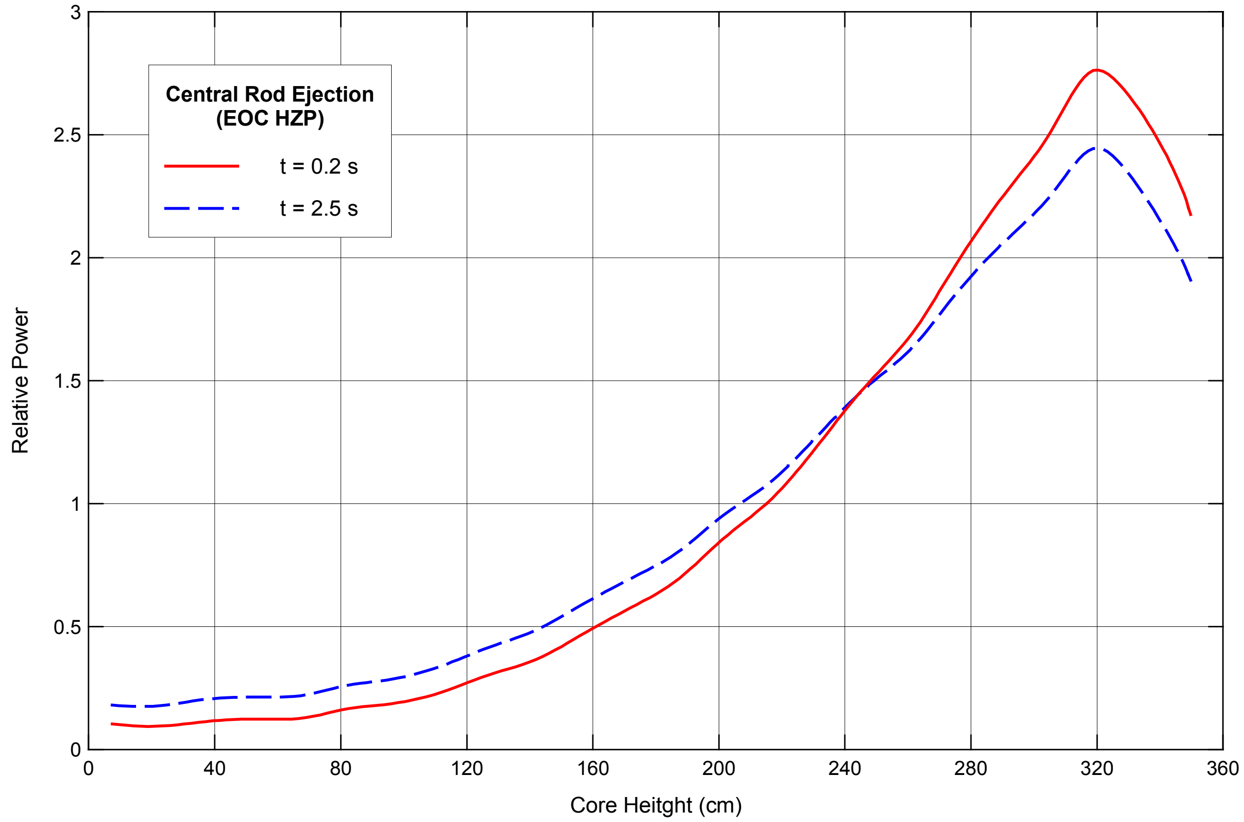

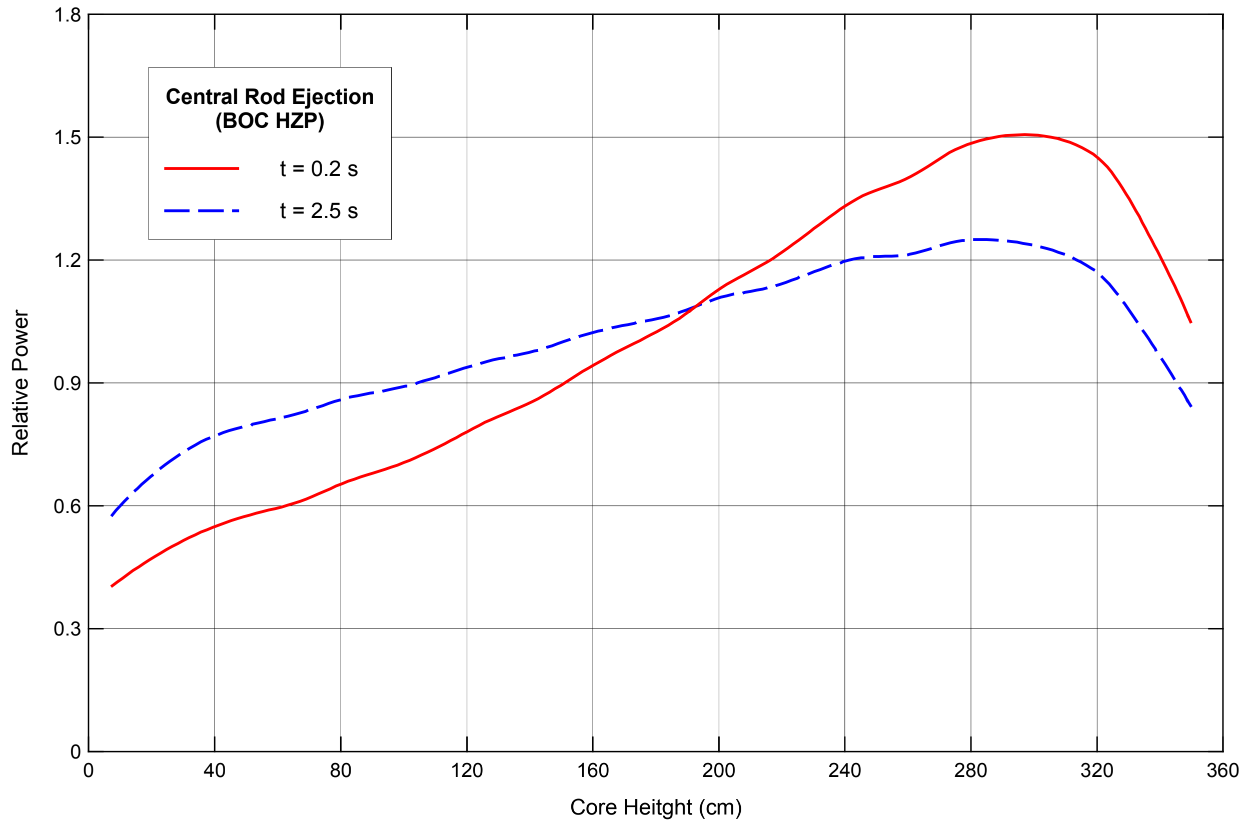

Figure 2.8. Average Axial Power Distribution (Cases EOC and BOC Centre)

Figures 2.9 through 2.16 presents the following parameters as a function of time of the transients: the core power, reactivity, and peaking factors for the first second, and the fuel temperature and fuel enthalpy increase for the hottest fuel pins. As can be seen in Figures 2.9-2.12, the power excursion starts at about 0.2 s. The power reaches a peak value at 0.24-0.34 s, then, due to negative reactivity feedback the power excursion is terminated.

The power pulse width is 62-65 ms at EOC and about 40 ms at BOC, thus, the power pulse (with the right boundary of 10% of a peak power) lies within 0.2-0.4 s at EOC and within 0.2-0.3 s at BOC. Reactivity reaches its maximum at 0.13-0.15 s due to withdrawal of the ejected rod and continues to be constant during about 0.10-0.15 s. Then reactivity begins to drop as a result of the negative reactivity feedback due to fuel heat-up and, later, due to coolant heat-up. At the time of the core peak power, reactivity is equal to approximately 1β. The behavior of the total power peaking factor, F_q, is rather similar: firstly it increases due to the rod ejection, then there is a “plateau” area with further decrease due to the core heat-up.

Figures 2.13 through 2.16 indicate that about 80% of the fuel enthalpy increase is produced during first 0.5-0.6 s after the rod ejection. It should be noted also that in the cases with ejection of the peripheral control rod, 50% of the core energy is produced only in several fuel assemblies: 17 at BOC and 23 at EOC, i.e. about 10-13% of the total number of fuel assemblies in the core (177).

Now consider an influence of spatial effects on the REA parameters. As it can be seen in Table 2.2 and Figures 2.9-2.16, noticeable differences in the power peak, fuel temperature and enthalpy increase occur. In the cases with ejection of the peripheral rod the peak power is lower then that in the cases with ejection of the central rod: by 2.5 times at EOC and by 2.9 times at BOC. On the other hand, practically the same, but inverse relationship occurs for the power peaking factor. The total core energy deposition can be characterized by a core-average fuel temperature increase. This parameter shows a similar tendency: corresponding ratio for the rod ejection cases is 2.2 at EOC and 2.6 at BOC. Consequently, it is worth to conclude that there is an evident correlation between the peak power, reactor energy deposition and the power peaking factor, F_q : the higher the F_q value, the lower the peak power and energy deposition in the core. However, it is clear, that a REA with the highest magnitude of F_q is more severe from the point of view of the local fuel enthalpy increase. Thus, in fact, the effect of the power peaking factor is revealed in two opposite directions, namely, a higher value of the peaking factor tends to decrease the total energy deposition in the core and, on the other hand, to increase the local fuel enthalpy.

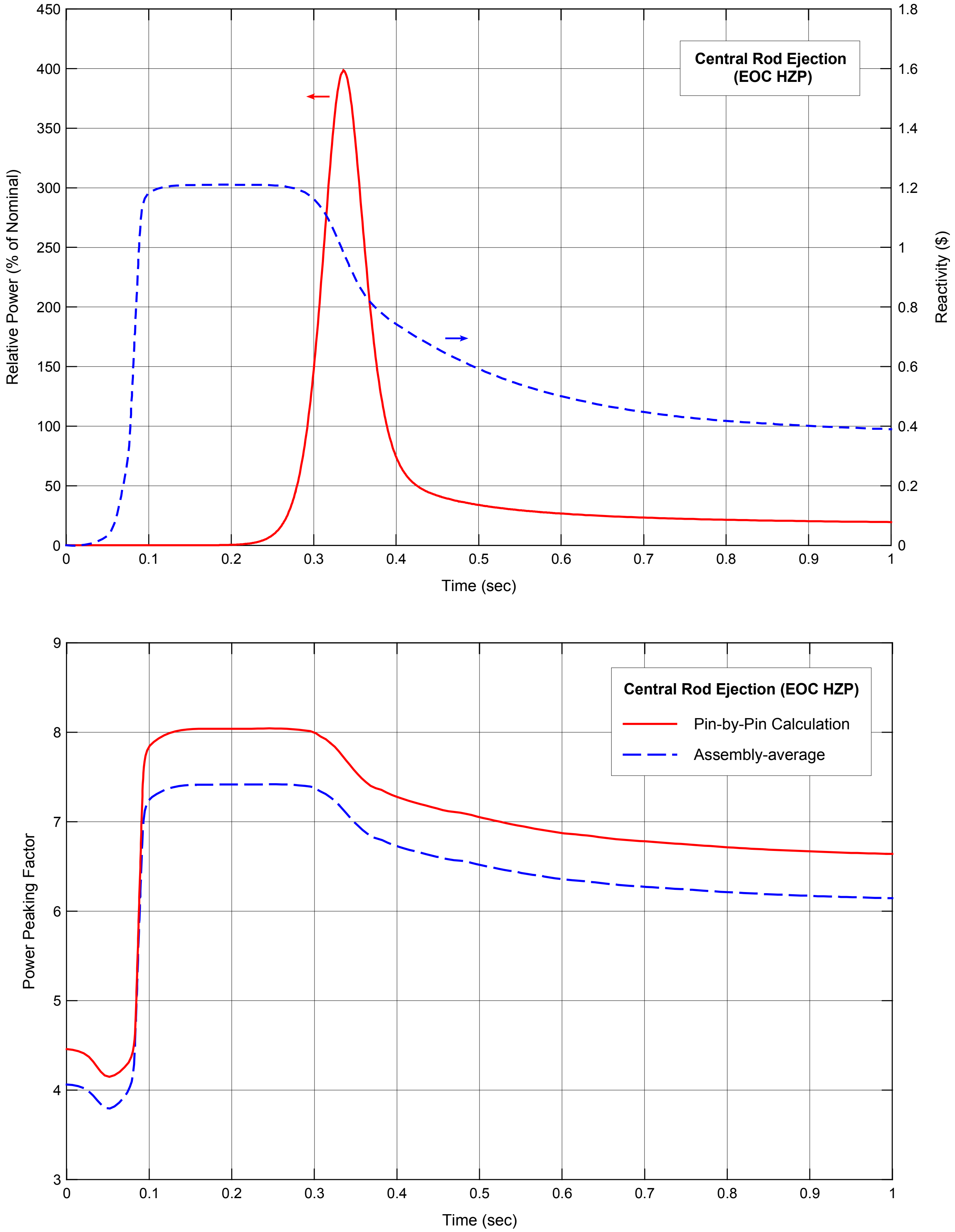

Figure 2.9. Power, Reactivity and Peaking Factors vs. Time (Case EOC Centre)

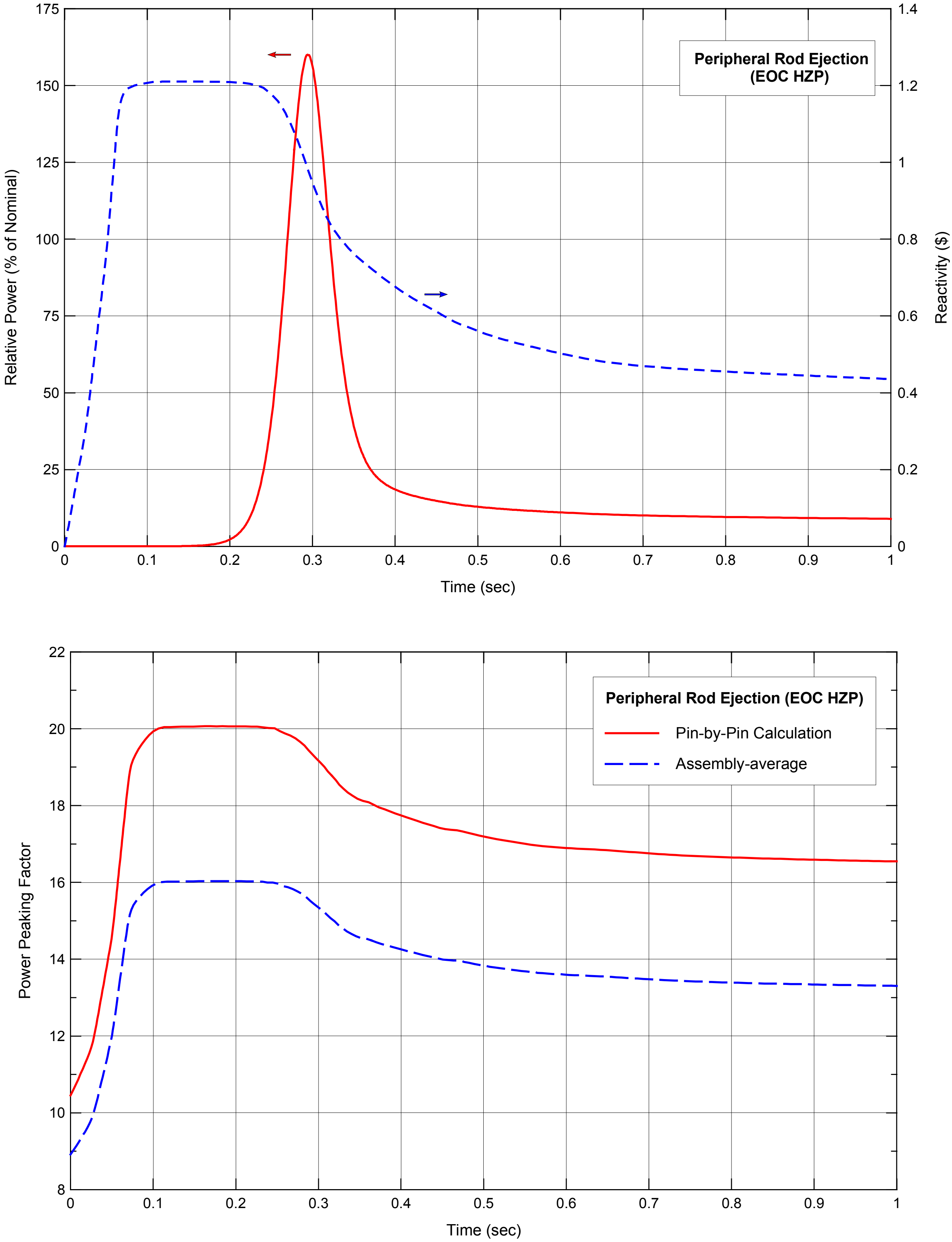

Figure 2.10. Power, Reactivity and Peaking Factors vs. Time (Case EOC Periphery)

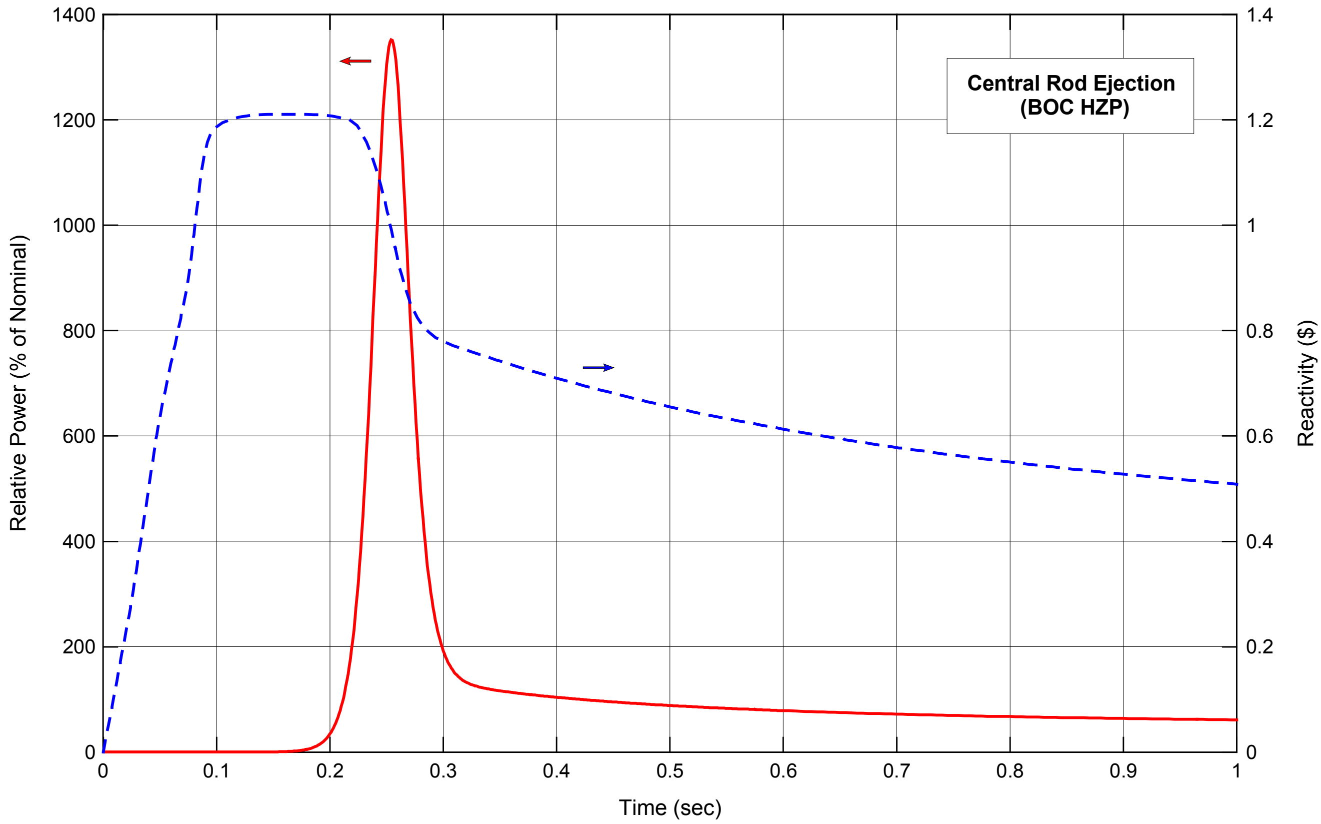

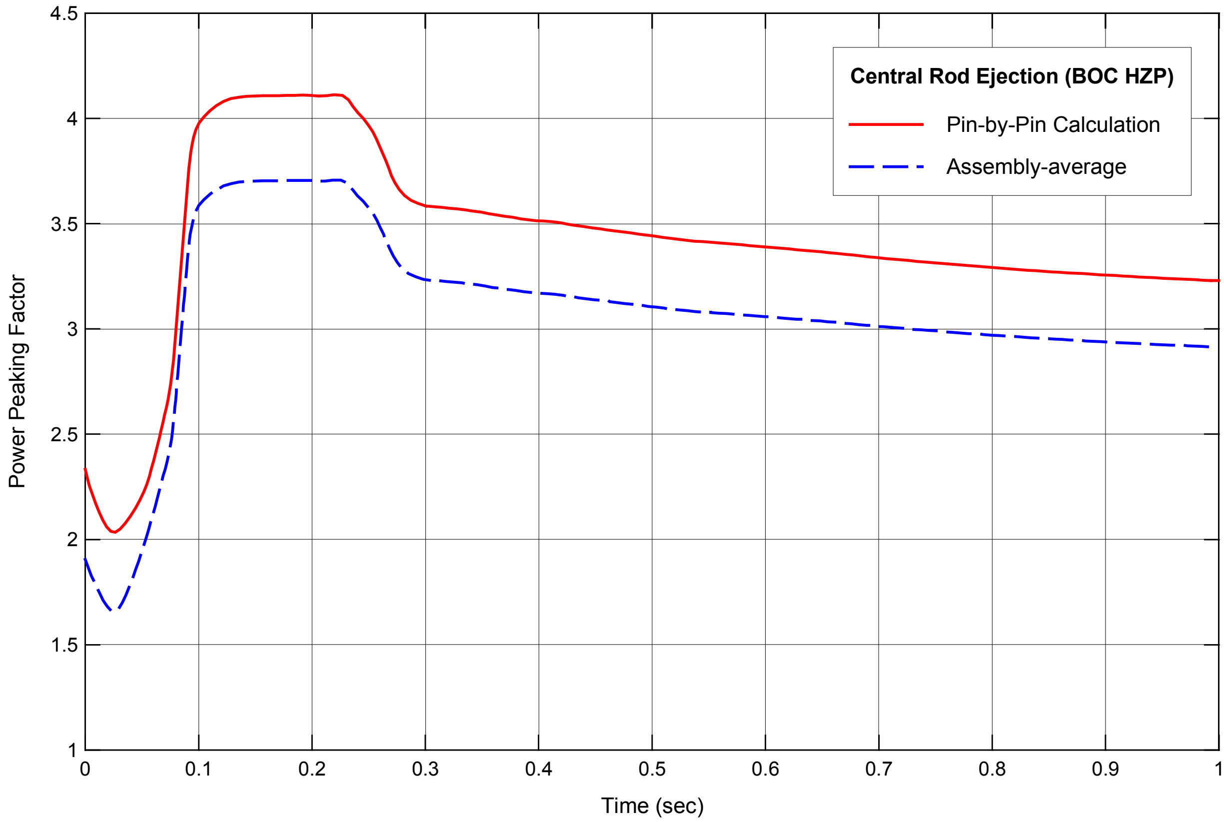

Figure 2.11. Power, Reactivity and Peaking Factors vs. Time (Case BOC Centre)

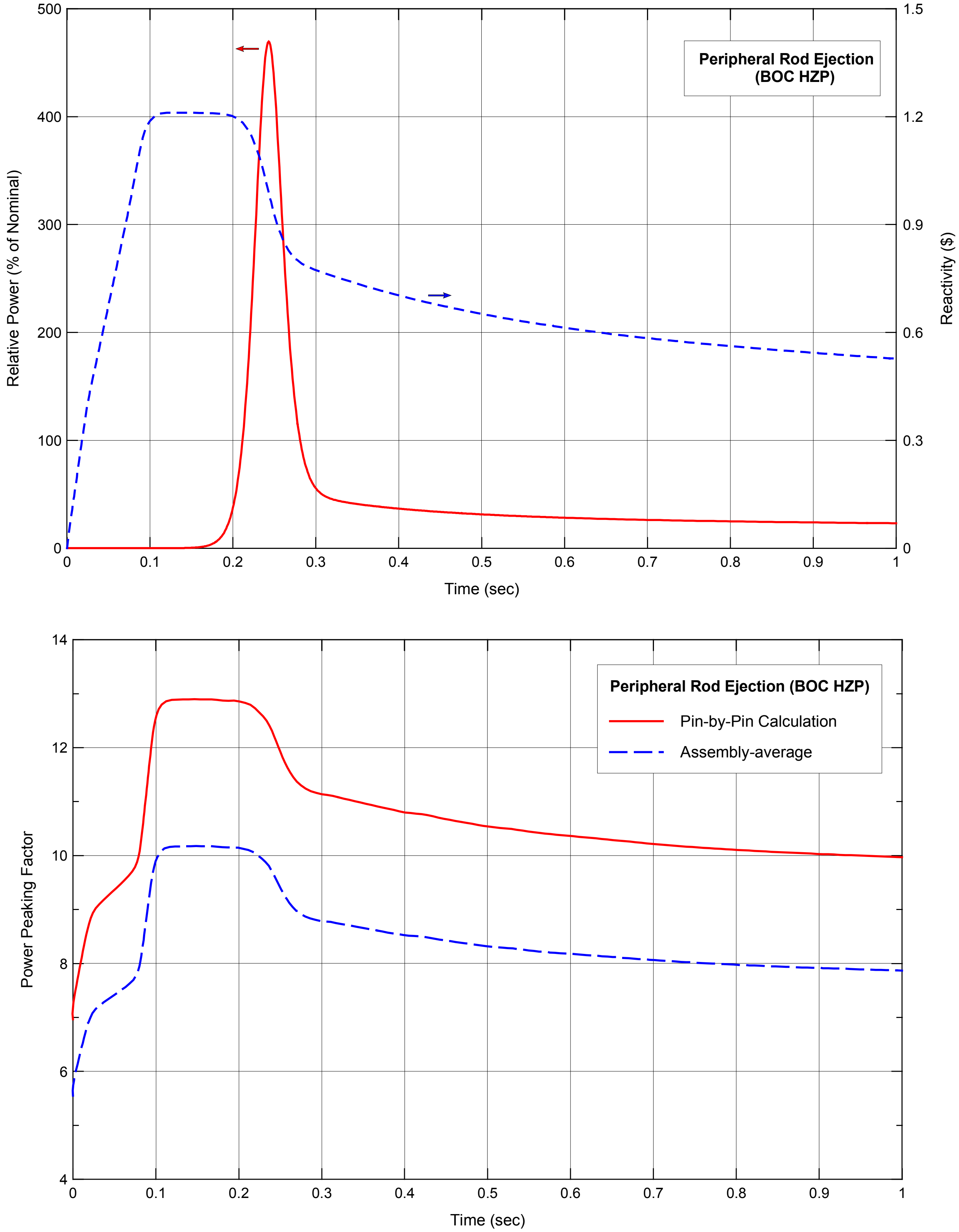

Figure 2.12. Power, Reactivity and Peaking Factors vs. Time (Case BOC Periphery)

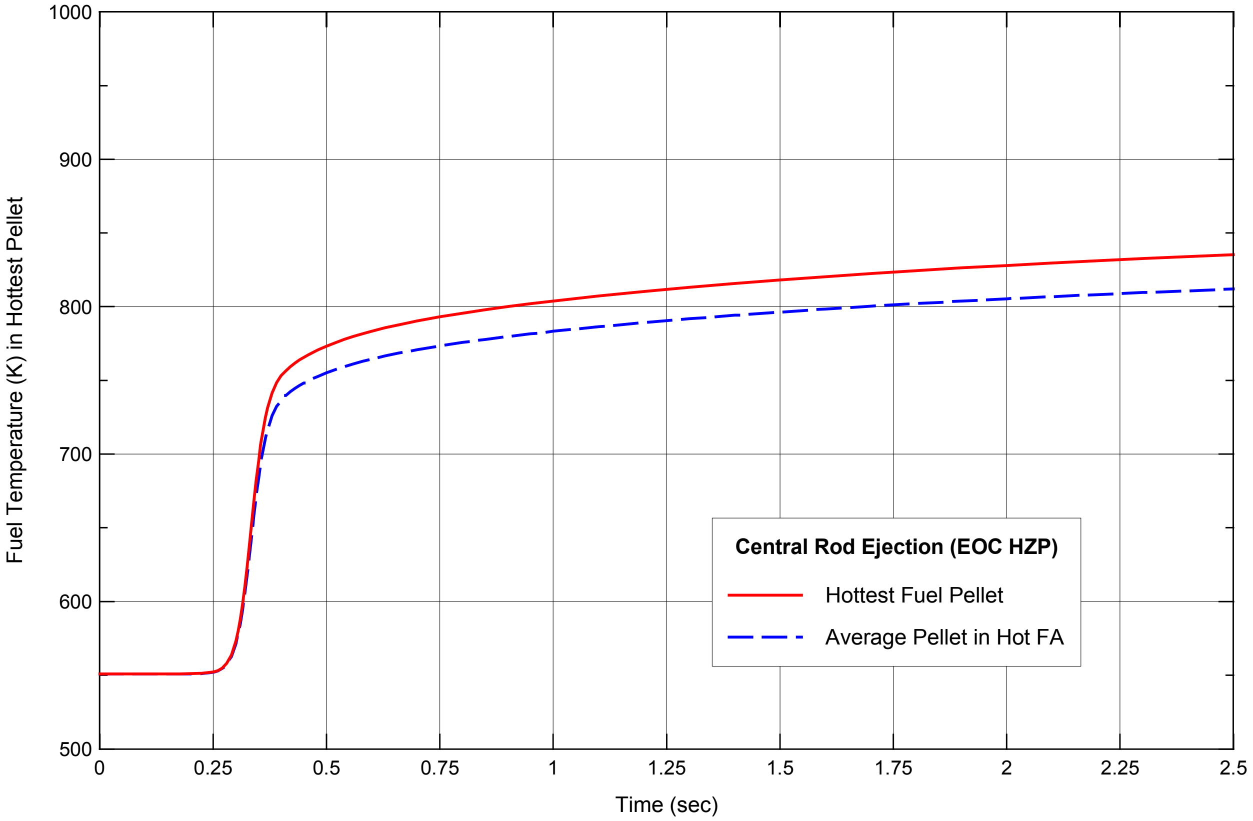

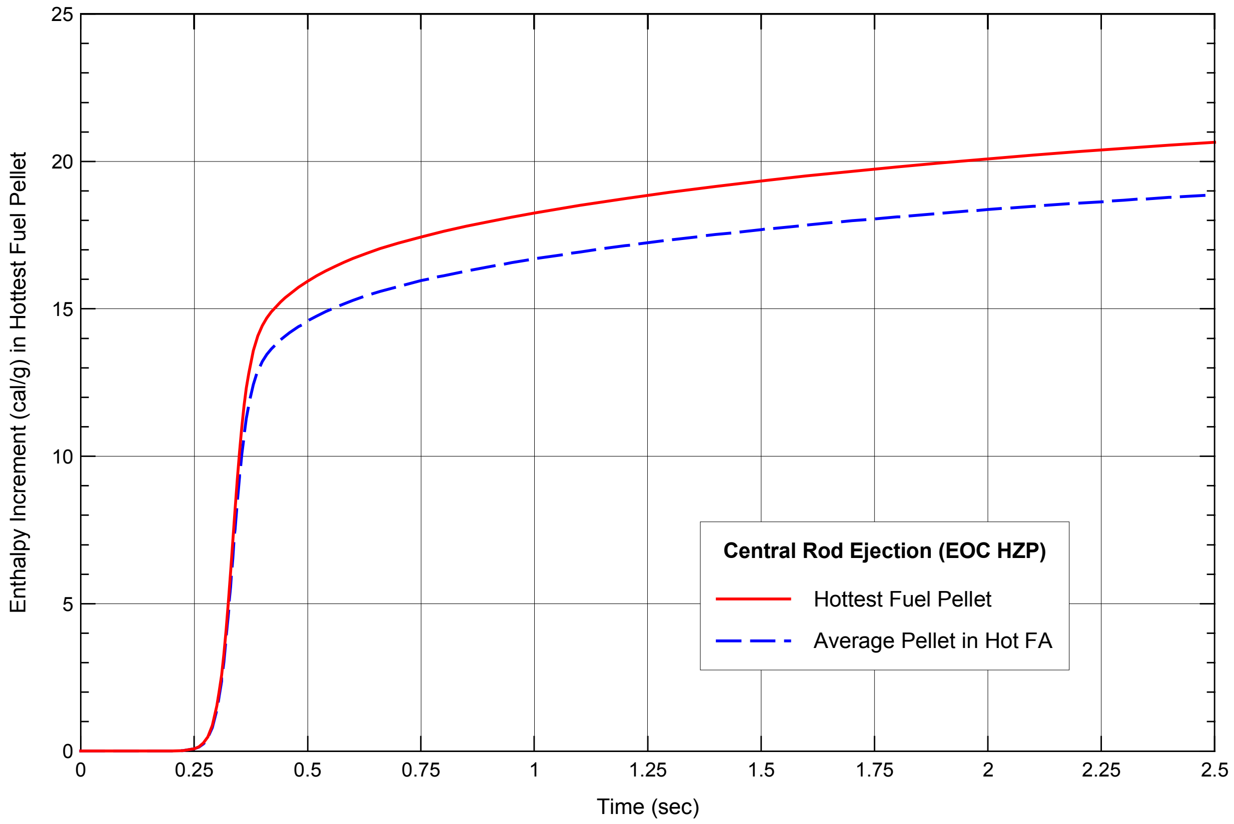

Figure 2.13. Fuel Temperature and Enthalpy in Hot Pins vs. Time (Case EOC Centre)

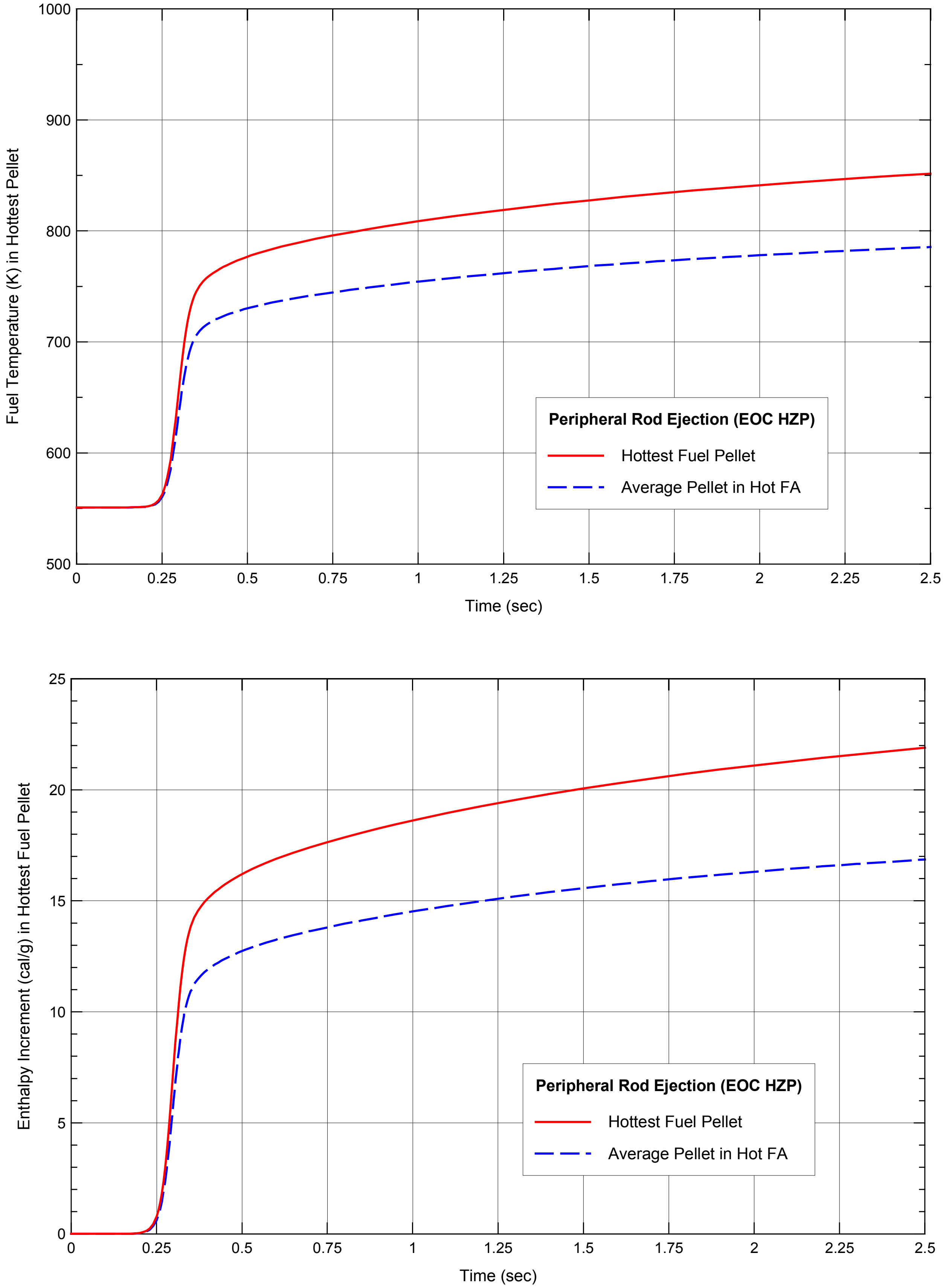

Figure 2.14. Fuel Temperature and Enthalpy in Hot Pins vs. Time (Case EOC Periphery)

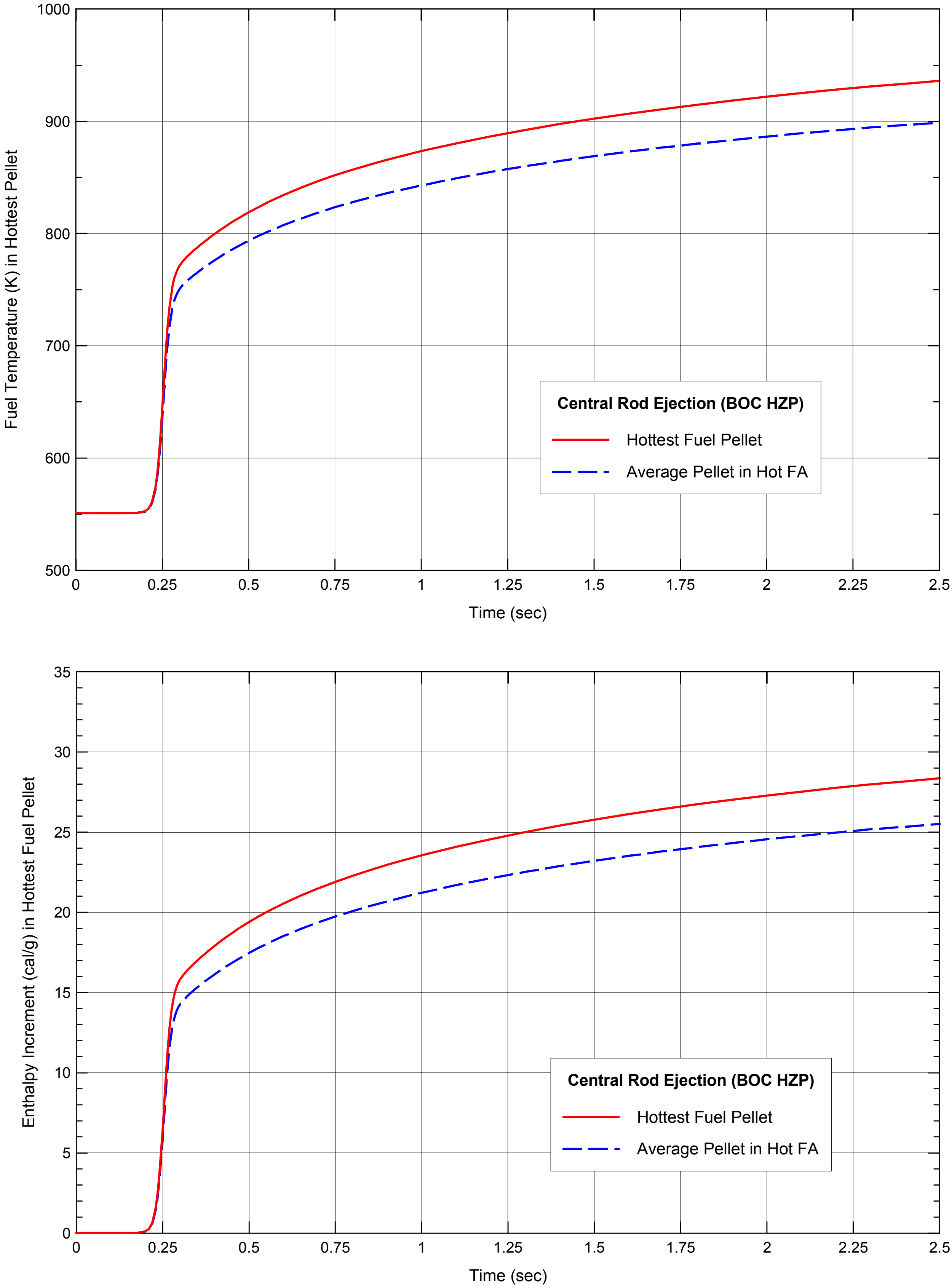

Figure 2.15. Fuel Temperature and Enthalpy in Hot Pins vs. Time (Case BOC Centre)

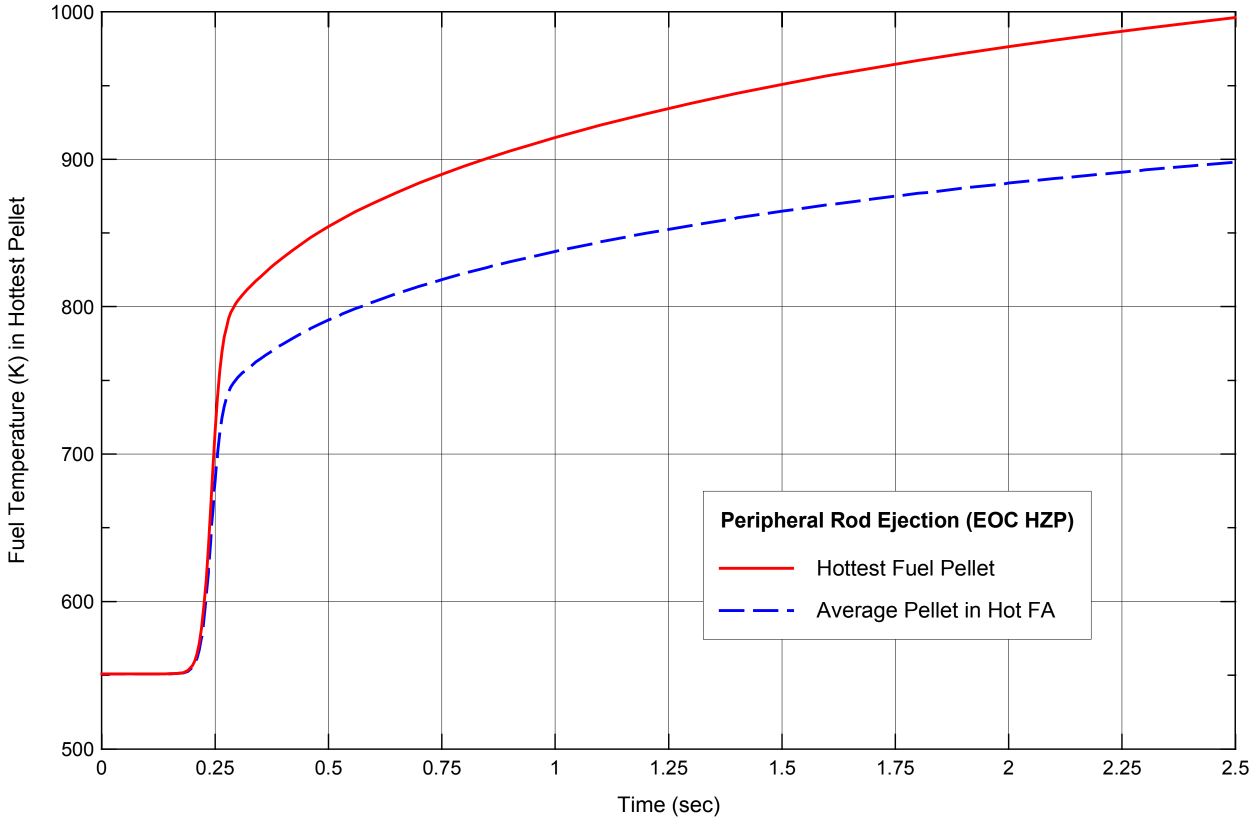

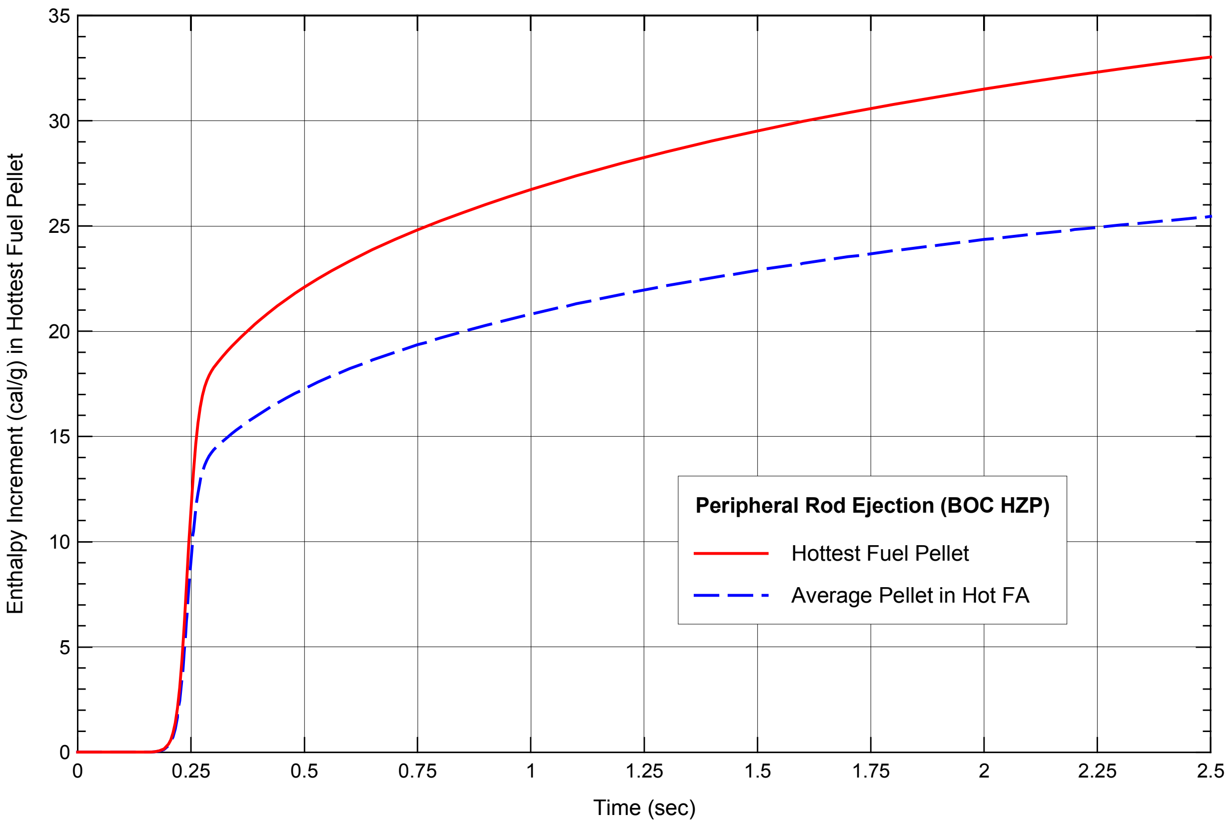

Figure 2.16. Fuel Temperature and Enthalpy in Hot Pins vs. Time (Case BOC Periphery)

As can be seen in Table 2.2 both cases with ejection of the peripheral rod show lower core-average fuel temperature compared with the cases with ejection of the central rod: 569 K at EOC and 595 K at BOC against 590 K and 664 K, respectively. Practically the same picture is observed for the peak assembly-average temperatures at EOC: 786 K against 812 K. But in the BOC cases they are very close: 899 K and 898 K. Consequently, the similar situation was found for the maximum assembly-average enthalpy increase: 16.9 cal/g against 18.9 cal/g at EOC, and about 25.5 cal/g in both BOC cases.

Therefore, from the point of view of assembly-by-assembly representation, both cases with ejection of the central control rod result in higher values of the assembly-average enthalpy increase compared with ejection of the peripheral rod. The next step is a definition of the hottest fuel pin. Consider the EOC cases. If this procedure is performed for the hottest fuel assembly, then we need the intra-assembly peaking factors for Assembly H9 (Case EOC Centre) and Assembly M12 (Case EOC Periphery). For both assemblies these factors were about 1.1. Thus, it can be expected the following values for the maximum pin enthalpy increase: 18.6 and 20.7 cal/g for ejection of the peripheral and central rod, respectively. As can be compared with the data presented in Table 2.2, such an approach leads to about 18% underestimation in the maximum pin enthalpy for Case EOC Periphery.

In the BOC cases the assembly-average parameters (the maximum fuel temperature and enthalpy) were found as approximately the same (899 K and 25.5 cal/g, respectively). The intra-assembly peaking factor was about 1.1 for Assembly H9 (Case BOC Centre) and about 1.27 for Assembly N13 (Case BOC Periphery). Thus, the maximum fuel pin enthalpy increase is estimated as 32.3 and 28.1 cal/g for ejection of the peripheral and central rod, respectively. The last values are close to those obtained from the pin-by-pin calculations (see Table 2.2).

Thus, the pin-by-pin calculations show that the peak fuel pin enthalpy increase is higher in both cases with ejection of the peripheral rod: 21.9 cal/g at EOC and 33.0 cal/g at BOC against 20.7 cal/g and 28.4 cal/g, respectively.

To investigate the influence of the power peaking factor on major REA parameters it is of interest to consider a simple approximation as described in the next section. This approach based on a Nordheim-Fuchs model [6], which is well-known and widely used for analytical estimations of different neutronic parameters in pulsed reactors.

3. NORDHEIM-FUCHS MODEL

This model is valid when the rod worth is greater than the value of the delayed neutron fraction, β. Next assumption is that the reactivity change due to feedback is proportional to the energy deposition. We will consider also an adiabatic approximation when there is no heat transfer to the coolant. Then using the point kinetics equations, the reactivity is:

$$\rho(t) = \rho_o - \gamma Q(t) \qquad (1)$$

where ρ_o is the reactivity worth of the ejected rod, γ is the feedback parameter, and Q(t) is the energy deposition. As it can be shown [6], the peak power, P_{max}, and the total energy deposition, Q_{tot}, are:

$$P_{max} = (\rho_o - \beta)^2 / (2\Lambda\gamma) \qquad (2)$$

and

$$Q_{tot} = 2\,(\rho_o - \beta) / \gamma \qquad (3)$$

where Λ is the prompt neutron lifetime. According to Eq. (1) the feedback parameter is:

$$\gamma = -\delta\rho / \delta Q \qquad (4)$$

where δQ is the energy deposition increase and $\delta\rho$ is the corresponding change in the reactivity. The adiabatic assumption means that the only feedback is the Doppler effect, thus, δQ and $\delta\rho$ can then be expressed in terms of the change in fuel temperature, ΔT:

$$\delta Q = \int_V C_p \,\Delta T \, dV \qquad (5)$$

and

$$\delta\rho = \langle \varphi^+, \alpha_D \,\Delta T \,\psi \rangle \qquad (6)$$

where C_p is the fuel heat capacity, V is the fuel volume in the core, φ^+ is the adjoint flux solution for the initial steady state, α_D is the fuel temperature (Doppler) reactivity coefficient, and ψ is the neutron flux with the following normalization condition:

$$<\varphi^+, \psi> = 1 \quad (7)$$

where the inner product represents integral over energy and the core volume. For further analysis it is worth to simplify both Eq. (5) and Eq. (6) if the fuel heat capacity and the Doppler coefficient are assumed to be constant. Such an approximation yields:

$$\delta Q = C_p V \Delta T_{avr} \quad (8)$$

and

$$\delta\rho = \alpha_D <\varphi^+, \Delta T\, \psi> \quad (9)$$

where ΔT_{avr} is the average change in fuel temperature over the core. In this case Eq. (4) can be expressed as:

$$\gamma = \gamma_o <\varphi^+, \Delta T\, \psi> / \Delta T_{avr} \quad (10)$$

where

$$\gamma_o = -\alpha_D / (C_p V)\ . \quad (11)$$

It can be seen that $\gamma = \gamma_o$ under the assumption of constant ΔT, i.e. $\Delta T = \Delta T_{avr}$. In other words it means that γ_o represents the feedback parameter in case when fuel temperature changes by the same value in each fuel pellet over the core. This is possible when power distribution is uniform in both radial and axial directions. It is obvious, that γ_o is the lower limit of the feedback parameter (α_D is always negative) and, thus, provides the maximum values of the peak power, P_{max}, and the total energy deposition, Q_{tot}, as seen from Eq. (2) and Eq. (3). To estimate the upper limit of γ, it is necessary to keep in mind that generally ΔT and weight functions φ^+ and ψ in Eq. (10) have quite different spatial distributions. Nevertheless, taking into account Eq. (7) the upper limit of the feedback parameter, γ_{max}, can be estimated as follows:

$$\gamma_{max} = \gamma_o \, \Delta T_{max} / \Delta T_{avr} \qquad (12)$$

where ΔT_{max} is the maximum change in fuel temperature over the core. $\Delta T_{max}/\Delta T_{avr}$ is the peaking factor for the change in fuel temperature. Under the adiabatic assumption, its value practically coincides with the power peaking factor, F_q. Then, the upper limit of γ is:

$$\gamma_{max} = \gamma_o \, F_q \ . \qquad (13)$$

Thus, both limits are proportional to the power peaking factor (taking into account that F_q is equal to 1 for the lower limit). Therefore, one can expect also that γ may be approximated as a linear function of F_q. In the present study, based on the RELAP-BARS calculations this evaluation was done. Figure 3.1 shows the relative feedback parameter, γ/γ_o, as a function of the pin-by-pin and assembly-average power peaking factors, F_q and F_q', respectively. As shown in the figure, both dependencies, $f(F_q)$ and $f(F_q')$, are approximately linear functions. More precise approximations for γ were found as follows:

$$\gamma \approx \gamma_o \, (0.38 \, F_q + 0.24) \qquad (14)$$

and

$$\gamma' \approx \gamma_o \, (0.50 \, F_q' - 0.09) \ . \qquad (15)$$

For the present analysis we can estimate the values of the feedback parameter, γ, during considered transients. At HZP conditions (T = 551 K) the value of the fuel heat capacity, C_p, is about 3.0 MJ/(m^3K). The fuel volume in the TMI-1 core is 9.2 m^3. The fuel temperature (Doppler) coefficient is about -2.8 pcm/K. Therefore, according to Eq. (11):

$$\gamma_o \approx 1.0 \times 10^{-6} \ \ MJ^{-1} \ . \qquad (16)$$

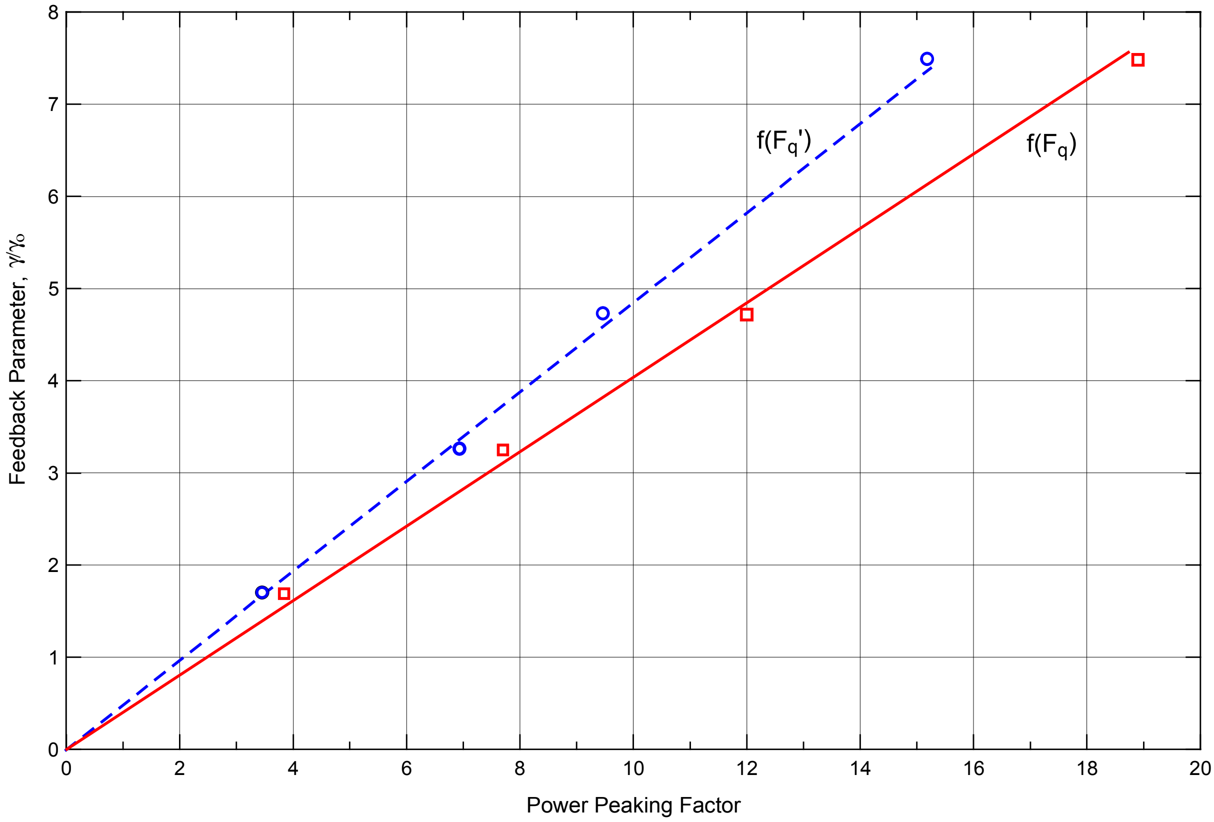

Figure 3.1. Feedback Parameter vs. Power Peaking Factor

This result was also confirmed by the RELAP–BARS calculation of Case EOC Centre under an assumption of the uniform heat-up over the core volume (i.e. when $\Delta T = \Delta T_{avr}$). Besides aforementioned peak power and total energy deposition, the power pulse width at the pulse half, $\Delta t_{1/2}$, can be estimated (within the Nordheim-Fuchs model) as follows:

$$\Delta t_{1/2} = 3.53\,\Lambda / (\rho_o - \beta) \quad . \qquad (17)$$

The Nordheim-Fuchs model does not take into account the effects of delayed neutrons. For this reason an applicability of this approach is restricted by the power pulse area. For the present study it means that this model is valid only to 0.4 s at EOC and to 0.3 s at BOC. Instead of the total energy deposition, Q_{tot}, as defined by Eq. (3), we will use the energy deposition at the power peak time, Q_o, which equals to $Q_{tot} / 2$. Table 3.1 presents some of the neutronic parameters of interest obtained from the RELAP–BARS calculations of the transients. The prompt neutron lifetime, Λ, feedback parameter, γ, and peaking factors, F_q and F_q', were averaged over those limits. The core energy deposition, Q_o, was defined as integral of the total core power up to the time of the power peak.

Table 3.1. Some Neutronic Parameters of REAs

Case Index $\rightarrow$	EOC Centre	EOC Periphery	BOC Centre	BOC Periphery
Core Energy Deposition, Q_o (GJ)	0.366	0.149	0.818	0.292
Prompt Neutron Lifetime, Λ (s)	1.86×10^{-5}	1.87×10^{-5}	1.46×10^{-5}	1.49×10^{-5}
Feedback Parameter, γ (MJ^{-1})	3.25×10^{-6}	7.48×10^{-6}	1.69×10^{-6}	4.72×10^{-6}
Pin-by-Pin Total Peaking Factor, F_q	7.70	18.9	3.84	12.0
Assembly-average Peaking Factor, F_q'	6.95	15.2	3.47	9.48

Using the data presented in Table 3.1 and the ejected rod worth (see Table 2.2) it is easy to evaluate the following parameters: P_{max}, Q_o, γ and $\Delta t_{1/2}$ by Eq. (2), (3), and (15)–(17). Table 3.2 contains these evaluated parameters.

Table 3.2. Evaluated Neutronic Parameters of REAs

Case Index $\rightarrow$	EOC Centre	EOC Periphery	BOC Centre	BOC Periphery
Peak Power (GW / % Nominal)	9.97 / 360	4.32 / 156	36.0 / 1300	12.6 / 456
Core Energy Deposition, Q_o (GJ)	0.338	0.147	0.789	0.282
Feedback Parameter, γ (MJ^{-1})	3.17×10^{-6}	7.42×10^{-6}	1.70×10^{-6}	4.80×10^{-6}
Feedback Parameter, γ' (MJ^{-1})	3.38×10^{-6}	7.51×10^{-6}	1.65×10^{-6}	4.65×10^{-6}
Power Pulse Width, $\Delta t_{1/2}$ (ms)	59.8	60.1	38.6	39.5

A comparison between the data presented in Table 3.2 with the calculated results (see Tables 2.2 and 3.1) shows that the peak power, P_{max}, and core energy deposition, Q_o, are underestimated by 3–10%. Practically the same uncertainties are found for the power pulse width, $\Delta t_{1/2}$. Both feedback parameters are estimated within 5% uncertainty. (It should be noted, that the approximations defined by Eq. (14) and Eq.(15) may differ for REAs with other neutronic parameters.)

Thus, these results confirm an assumption about strict correlation between the peak power, core energy deposition and as a result, fuel temperature (or enthalpy) increase, and the power peaking factor. Presented simplified estimations allow to conclude the following fact: the feedback parameter, γ, is approximately proportional to the power peaking factor. In its turn, both the peak power and energy deposition is inversely proportional to γ and, as a result, to the power peaking factor.

Therefore, it may be concluded that if the adiabatic assumption were valid during a REA, it would be expected that the peak fuel enthalpy increase practically does not depend on spatial effects. In other words, in the transients with quite different power distributions in the radial and axial directions, but with the same neutronic parameters, ρ_o and β, the results for the peak fuel enthalpy increase are to be obtained as very similar.

Of course, a REA may be considered as an adiabatic process in terms of energy deposition only within a narrow time interval limited by the power pulse area when a very fast rise and decrease of power takes place. When power decreases to about 10% of its peak value, effects of delayed neutron become distinct. After the power pulse, the energy deposition process is rather mild. During the present study with 1.21β REAs it was found the following. Just after the termination of the power pulse (at 0.4 s at EOC or 0.3 s at BOC) about 3-4% of fuel energy release is transmitted to the coolant; this value becomes about 20% at 1 s. Besides, the prompt fraction of energy deposition (within the limits of the power pulse when the adiabatic assumption is valid) gives only about 30-40% of the total energy deposition at the end of the transient. On this evidence, it is clear that the above reasoning should be considered as very approximate. It should be also to take into account that the feedback parameter, γ, changes by several times during the transient as calculated by RELAP-BARS. As it can be seen in Figures 2.13 and 2.14 for the EOC cases, the difference between the assembly-average fuel enthalpy increase reaches 10% already at 0.4 s. From the other hand, as shown in Figures 2.15 and 2.16, for the BOC cases this difference is very small. Nevertheless, above mentioned simplified approach may be very useful to estimate some important parameters of a REA.

4. RESULTS OF STEADY-STATE ROD WORTH CALCULATIONS

Recently an intercomparison of PWR REA calculations performed by different codes has been carried out [5]. In the framework of this study a number of steady-state calculations were done using the following neutronic codes: BARS [1], PARCS [7] and CRONOS2 [8], developed in the Russian Federation, the United States, and France, respectively. PARCS and CRONOS2 are assembly-by-assembly nodal diffusion codes. During that study they used the same two-group cross-sections generated with the CASMO-3 code. BARS used four-group lambda-matrices generated with the TRIFON code. The reactor model was the same as defined in Section 2 for Case EOC Centre (see also Figure 2.1).

Among those steady-state calculations there were calculations of each control rod in Bank 7 at HZP conditions. Table 4.1 presents the results of the steady-state calculations of the rod worths. Last column indicates average deviations of the BARS data from the PARCS and CRONOS2 results. Comparison of the rod worths shows that the differences between the PARCS and CRONOS2 results do not exceed 3%. The BARS result is slightly higher for Rod H8 (by 1%); the deviation for Rod H12 is 8%. The most deviation was found for Rod N12 (about 35%).

The same steady-state calculations but at BOC HZP conditions (see Figure 2.2) have been performed by the PARCS code [9]. Table 4.2 presents those results in comparison with the BARS data. As can be seen in Table 4.2, the most deviations occur for Rod H8 (18%) and Rod N12 (15%). The deviation for Rod H12 (9%) is practically the same as was found for EOC HZP case.

From a comparison of the data presented in Tables 4.1 and 4.2, the following observations can be obtained. The BARS results indicate that the heaviest rod (Rod N12) has a similar worth in terms of delayed neutron fraction, β, (about 0.9β) in both cases (at BOC its worth is 16% higher in absolute units). The PARCS results show that at BOC conditions the worth of Rod N12 is higher by 14% in absolute units and by 39% in terms of β.

Nevertheless, 0.91β worth seems to be the highest one. For this reason to reach a prompt critical (i.e. a rod worth of more than 1β) in reality it is necessary to change the initial control rod arrangement in the core. If Rod M11 of Bank 5 is assumed to be stuck-out at the upper position (i.e. out of the core), the worth of Rod N12 can be significantly increased. As the BARS steady-state calculations show, the worth of Rod N12 is as follows:

- 907 pcm or 1.74 β at EOC HZP conditions;
- 954 pcm or 1.51 β at BOC HZP conditions.

Table 4.1. Steady-State Calculational Results for EOC HZP Case

Parameter	BARS	PARCS	CRONOS2	Deviation
Worth of Rod H8 (pcm/β)	349 / 0.670	347 / 0.666	345 / 0.662	3 / 0.006
Worth of Rod H12 (pcm/β)	204 / 0.391	188 / 0.361	188 / 0.361	16 / 0.030
Worth of Rod N12 (pcm/β)	473 / 0.907	344 / 0.660	353 / 0.677	125 / 0.240

Table 4.2. Steady-State Calculational Results for BOC HZP Case

Parameter	BARS	PARCS	Deviation
Worth of Rod H8 (pcm/β)	273 / 0.432	230 / 0.363	43 / 0.069
Worth of Rod H12 (pcm/β)	164 / 0.259	150 / 0.237	14 / 0.022
Worth of Rod N12 (pcm/β)	548 / 0.867	477 / 0.754	71 / 0.113

The situation when a single control rod of any regulating bank is found as stuck-out at the upper or intermediate position, is possible as a result of any control system malfunction during a rector trip. Then if a reactor reaches a critical level at HZP, ejection of a control rod neighboring with a stuck rod may lead to a prompt critical.

In conclusion it should be noted that 35% uncertainty in the rod worth as was found during the aforementioned intercomparison between the PARCS and BARS steady-state results (see Table 4.1), may lead to a significant uncertainty in consequences of a REA, especially if the ejected rod worth is above 1β. For instance, in a 1.2β REA a 35% uncertainty in the ejected rod worth may results in about 300% uncertainty in the core energy deposition and, consequently, in the peak fuel enthalpy increase, as it can be seen from Eq. 3 presented in the previous section.

5. CONCLUSIONS

This study was undertaken to analyze spatial effects in the course of rod ejection accidents. If the rod worth is sufficient to reach prompt critical i.e. greater than β, then its withdrawal initiates a fast power excursion which is terminated due to the negative reactivity feedback. This event is of interest from the point of view of prediction of the maximum increase in fuel enthalpy during the accident. Although, as numerous steady-state calculations show, the maximum value of control rod worth scarcely exceeds 1β in a PWR, such an accident is to be considered in a NPP safety analysis with conservatively increased value of the ejected rod worth.

A key parameter of interest in a NPP safety analysis is the peak local fuel enthalpy, which establishes the acceptance criterion for unacceptable fuel damage in reactivity initiated accidents in a LWR. It is well-established that spatial effects play an important role in the REA consequences, in particular, the core peak power and energy deposition which can be approximately related to the fuel enthalpy rise under an adiabatic assumption (no heat transfer from the fuel to the coolant). Then using simplified analytical approximations it is easy to establish relationships between the major parameters of interest and spatial effects. To characterize them during the transient, the power peaking factors, F_q and F_q' are used: the former is related to the pin-by-pin representation of the core power, and the latter – with the assembly-by-assembly one.

An influence of spatial effects on the REA parameters is revealed in two opposite trends. On the one hand, the higher the power peaking factor, the higher the local fuel enthalpy. On the other hand, a higher value of F_q tends to slow down the total energy deposition in the core and, as a result, to mitigate the fuel enthalpy increase. This is due to the fact that the fuel and moderator feedback is stronger in the hottest regions of the reactor core and reduces the peak power and reactivity.

In this study an analysis of REAs was carried out using the REALP–BARS code [1], which allows a 3-D pin-by-pin neutronic and assembly-by-assembly thermal-hydraulic simulation of a LWR. Four REAs with ejection of the central or peripheral control rod at the EOC or BOC initial conditions were analyzed using a PWR calculational model based on TMI-1. The same EOC PWR model was used during the previous analysis, thus, the present study may be considered as a further extension of the previous calculational analysis of the TMI-1 REA using different methods from USA, France and Russian Federation [5].

To provide identical initial conditions the worth of an ejected control rod was artificially fitted to 1.211β for all cases. Duration of the transient was limited by 2.5 s. An assembly-average representation of fuel and coolant parameters with 24 nodes in an axial direction was used to treat the core thermal-hydraulics. A separate heat structure was chosen to represent the hottest fuel pin in the reactor core (the coolant parameters were the same as for that fuel assembly where the hottest pin was located).

The calculational results showed that the peak powers were different to a great extent: from 4.4 to 37.5 GW. In the cases with ejection of the peripheral rod, the peak power was lower compared with ejection of the central rod by 2.5 times at EOC and by 2.9 times at BOC. In turn, practically the same, but inverse relationship was found for the power peaking factors. The maximum assembly-average fuel temperatures were very close (within about 1 K) for the BOC cases. Corresponding values for the maximum fuel enthalpy increase were about 25.5 cal/g. For the EOC cases those values differed by 2 cal/g (18.9 and 16.9 cal/g for the cases EOC Centre and EOC Periphery, respectively). Thus, from the point of view of the assembly-by-assembly representation, the central rod ejection accidents with rather small power peaking factors resulted in slightly higher values of the maximum fuel enthalpy increase. On the contrary, the pin-by-pin representation showed that the peak local fuel enthalpy was higher for the peripheral REAs with the highest power peaking factors. In the EOC cases, a higher value of the peak enthalpy was due to the fact that the hottest fuel pin was found in Assembly N13 (see Figure 2.5) diagonally adjacent to the hot assembly M12. This fact indicates that a problem of proper definition of the hottest pin location is essential. In the considered case the incorrect definition of the hottest pin location using an assembly-by-assembly approach, can lead to 15%-underestimation in the peak local enthalpy rise. Therefore, uncertainties of such a kind should be taken into account in an uncertainty analysis of the reactivity initiated accidents in LWRs.

The point kinetics approximation within the Nordheim-Fuchs model allowed to derive simple relationship between the peak power, total energy deposition and the power peaking factor. It was found that in the framework of this model the peak power and total energy deposition are inversely proportional to the power peaking factor. Thus, if assume that the peaking factor for fuel enthalpy increase coincide with that for power, then it can be expected that the maximum assembly-average fuel enthalpy increase is practically independent on spatial effects.

In spite of the fact that the Nordheim-Fuchs model is valid only within a narrow time interval limited by the power pulse area, this simplified approach (with the point kinetics parameters evaluated in advance) may be successfully used, in particular, for estimation of the major parameters of REAs.

Another important problem of a REA analysis deals with uncertainty in prediction of the rod worth by different calculational methods. As was found during this study, the BARS results for the rod worths were always higher compared with those calculated by the PARCS code. The most difference occurs for the peripheral rod N12 (see Figures 2.1 and 2.2) nearest to the reflector region. At the EOC initial conditions this difference reaches 35%. A nature of this discrepancy may be explained definitively by additional intercomparison with other results obtained using, in particular, codes of more precise calculational methods.

It should be mentioned, that as the steady-state calculations of the rod worths show, 0.91β worth seems to be the highest one, which does not allow to reach a prompt critical. Thus, to provide desired 1.2β rod worth it is necessary to adjust artificially neutronics parameter of the ejected rod. Another way, which is more realistic in comparison with the previous one, is to assume that there is a stuck rod near the ejected control rod. For instance, in the case of ejection of the peripheral rod N12 (with stuck rod M11) the inserted reactivity value may reach 1.74β at EOC HZP conditions.

In summary, the objective of this study was to understand the role of spatial effects in the course of different rod ejection accidents. The influence of spatial effects may be of interest not only in an analysis of reactivity initiated events, but also in interpretation of in-pile burst tests aimed to understand fuel rod behavior under severe accidents. The present study has also looked at the effect of the calculational approach (pin-by-pin against assembly-by-assembly) on the major parameter of a REA – the peak local enthalpy increase.

6. REFERENCES

1. A. Avvakumov, V. Malofeev, and V. Sidorov, “Analysis of Pin-by-Pin Effects for LWR Rod Ejection Accident,” NUREG/IA-0175, NSI RRC KI 90-12/1-3-00, IPSN/00-13, 2000
2. K. N. Ivanov, et al., “Pressurized Water Reactor Main Steam Line Break (MSLB) Benchmark; Volume I: Final Specifications,” U.S. Nuclear Regulatory Commission and OECD Nuclear Energy Agency, NEA/NSC/DOC(99)8, April 1999
3. N. K. Todorova and K. N. Ivanov, “Project Report on Task 1 of BNL Sub-Contract “Core Model – PARCS/RELAP5,” The Pennsylvania State University, 2000
4. A. Avvakumov, et al., “3-D Pin-by-Pin Modeling of Rod Ejection RIA in VVER-1000,” Nuclear Safety Institute of Russian Research Centre “Kurchatov Institute”, Report No. 90-12/1-33-97, 1997
5. D. J. Diamond, et al., “Intercomparison of Results for a RWR Rod Ejection Accident,” Nuclear Engineering and Design, **208**, 2001
6. G. Bell and S. Glasstone, “Nuclear Reactor Theory,” Van Nostrand Reinhold Company, 1970
7. H. G. Joo, et al., “PARCS: A Multi-Dimensional Two-Group Reactor Kinetics Code Based on the Non-linear Analytic Nodal Method,” PU/NE-98-26, Purdue University, School of Nuclear Engineering, September, 1998
8. J.-J. Lautard, S. Loubière, C. Fedon-Magnaud, “CRONOS2, A Modular Computational System for Neutronic Core Calculations,” IAEA Specialist Meeting on Advanced Calculations Methods for Power Reactors, Cadarache, France, 1990
9. B. P. Bromley, Memo to D. J. Diamond, Brookhaven National Laboratory, May 2, 2001

APPENDIX A

CALCULATIONAL RESULTS FOR A REA WITH INCREASED ROD WORTH

As it was above mentioned, the BOC delayed neutron fraction was approximately 21% higher compared with that at the EOC conditions (632 pcm against 521 pcm). This means that at the same relative rod worth expressed in terms of β, there are two different absolute values of the rod worth at BOC and EOC. For instance, for a 1.21β rod worth the absolute values are 631 pcm and 765 pcm at EOC and BOC, respectively. In this respect it would be interesting to compare the results for EOC REA with the same absolute value of the rod worth as at BOC, i.e. 765 pcm (1.47β).

This section contains the calculational results of a REA with ejection of the central rod with increased worth obtained by the RELAP–BARS code. The absolute value of the rod worth corresponds to that presented in Table 2.2 for the BOC cases, i.e. 765.7 pcm or 1.47β in terms of the EOC delayed neutron fraction. The reactor model and the accident scenario were the same as described in Section 2. To provide required 1.47β, the initial arrangement of the control rod banks was changed. As was found it was impossible to obtain such a high reactivity only by changing neutronic parameters of the ejected rod. For this reason, four control rods of Bank 2 located at Assembly K9 diagonally adjacent to Assembly H8 were partly inserted before the REA (see Figure 2.1). Then they were also withdrawn together with the ejected rod H8 with the same speed.

Table A.1 summarizes the calculational results of 1.47β EOC transient with ejection of the central control rod. Figures A.1 and A.2 show the following parameters as a function of time of the transient: the core power, reactivity, fuel temperature, and fuel enthalpy increase for the hottest fuel pin.

The power pulse, as can be seen in Figure A.1, is very narrow, the pulse width is less than 30 ms. The power excursion produces rapidly the core heat-up, and due to the negative fuel and moderator temperature feedback, is terminated. As a result of the strong feedback, the reactivity drops up to 0.06β (against 0.3-0.4β in 1.21β transients) at about 0.7s. After a while the reactivity becomes to rise as a result of the positive reactivity insertion due to the core cooldown. (This effect was not observed during the 1.21β REA analysis, nevertheless, as was reported in [5], the Doppler and moderator reactivity effects were of the same order.

Table A.1. Calculational Results for 1.47β EOC REA

Parameter	Value
Ejected Rod Worth (pcm / β)	765.7 / 1.4695
Peak Power (GW / % Nominal)	48.83 / 1762
Time of Peak Power (ms)	206.4
Power Pulse Width (ms)	29.5
Maximum Core-Average Fuel Temperature (K)	610.6
Maximum Fuel Assembly Temperature (K)	960.5
Maximum Fuel Pin Temperature (K)	995.1
Maximum Assembly Enthalpy Increase (cal/g)	30.27
Maximum Pin Enthalpy Increase (cal/g)	32.96
Time of Maximum Pin Enthalpy Increase (ms)	507.0
Position of the Hottest Assembly	H9
Position of the Hottest Fuel Pellet (Axial Layer)	H9 (Node 22)

It is obvious that sooner or later the negative moderator feedback component becomes to decrease due to forced circulation of the coolant with the core inlet temperature of 551 K.)

As can be seen in Figure A.2 the fuel temperature/enthalpy reaches a peak value at about 0.5 s, then gradually decreases. The maximum fuel pellet temperature is 995 K, which corresponds to the enthalpy increase of 33 cal/g. The last value is higher by about 60% in comparison with Case EOC Centre, i.e. 1.21β REA (see Table 2.2). This is in contrast to the simplified estimation: according to Eq. 3 it should be expected at least twice as high (or more precisely, about 46 cal/g).

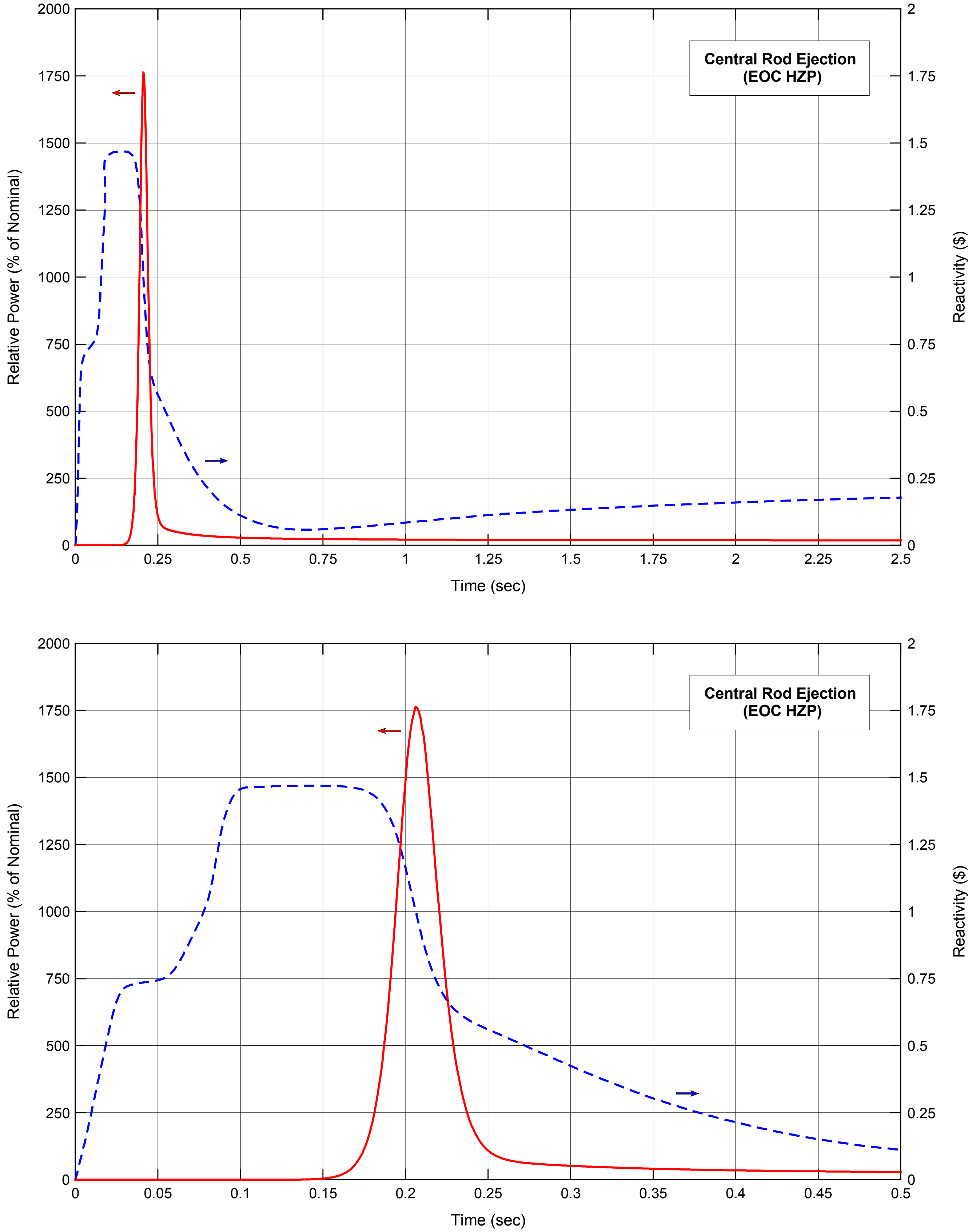

Figure A.1. Power and Reactivity vs. Time

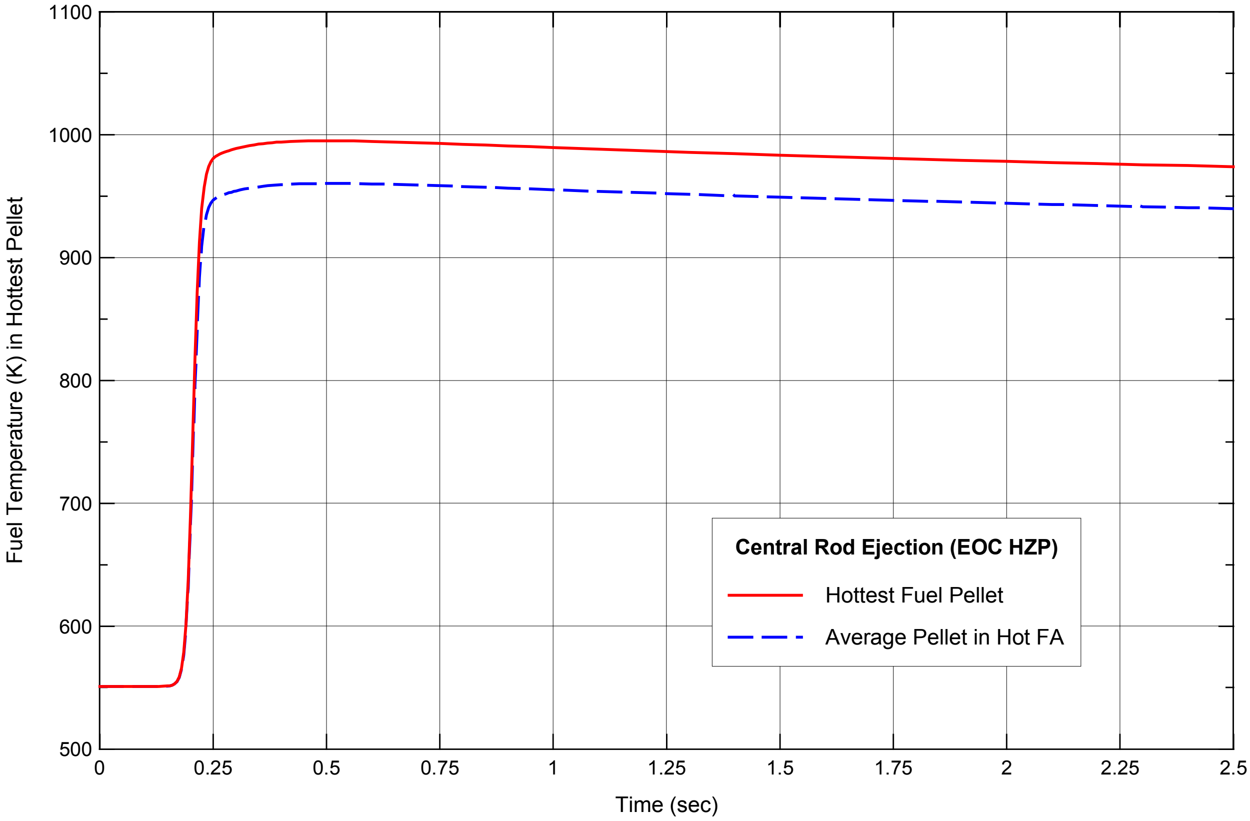

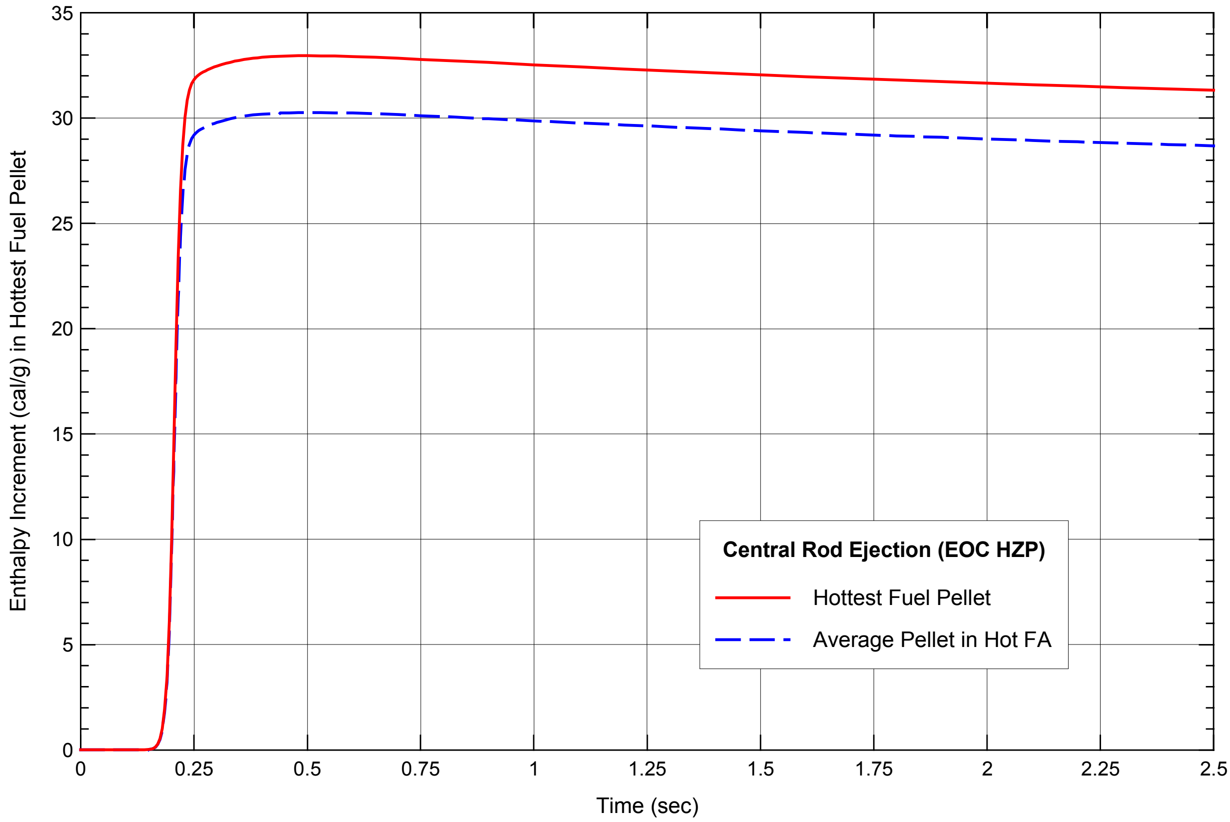

Figure A.2. Fuel Temperature and Enthalpy in Hot Pins vs. Time